BH9, a New Comprehensive Benchmark Dataset for Barrier Heights and Reaction Energies: Assessment of Density Functional Approximations and Basis Set Incompleteness Potentials

Viki Kumar Prasad,[1, *] Zhipeng Pei,[1] Simon Edelmann,[1, †] Alberto Otero-de-la-Roza,[2, ‡] and Gino A. DiLabio[1, §]

[1]*Department of Chemistry, University of British Columbia,*
3247 University Way, Kelowna, British Columbia, Canada V1V 1V7
[2]*Departamento de Química Física y Analítica and MALTA Consolider Team,*
Facultad de Química, Universidad de Oviedo, 33006 Oviedo, Spain
(Dated: November 29, 2021)

The calculation of accurate reaction energies and barrier heights is essential in computational studies of reaction mechanisms and thermochemistry. In order to assess methods regarding their ability to predict these two properties, high-quality benchmark sets are required that comprise a reasonably large and diverse set of organic reactions. Due to the time-consuming nature of both locating transition states and computing accurate reference energies for reactions involving large molecules, previous benchmark sets have been limited in scope, the number of reactions considered, and the size of the reactant and product molecules. Recent advances in coupled-cluster theory, in particular local correlation methods like DLPNO-CCSD(T), now allow the calculation of reaction energies and barrier heights for relatively large systems. In this work, we present a comprehensive and diverse benchmark set of barrier heights and reaction energies based on DLPNO-CCSD(T)/CBS, called BH9. BH9 comprises 449 chemical reactions belonging to nine types common in organic chemistry and biochemistry. We examine the accuracy of DLPNO-CCSD(T) vis-a-vis canonical CCSD(T) for a subset of BH9 and conclude that, although there is a penalty in using the DLPNO approximation, the reference data are accurate enough to serve as benchmark for density-functional theory (DFT) methods. We then present two applications of the BH9 set. First, we examine the performance of several density functional approximations commonly used in thermochemical and mechanistic studies. Second, we assess our basis set incompleteness potentials regarding their ability to mitigate basis set incompleteness error. The number of data points, the diversity of the reactions considered, and the relatively large size of the reactant molecules make BH9 the most comprehensive thermochemical benchmark set to date, and a useful tool for the development and assessment of computational methods.

INTRODUCTION

The prediction of barrier heights (BHs) and reaction energies (REs) using computational methods, combined with the application of transition-state theory,[1–3] is a powerful tool for the elucidation of reaction mechanisms in chemistry.[4,5] The prediction of kinetic and thermochemical properties is also important in biochemistry, and has contributed greatly to the understanding of the catalytic activity of enzymes,[6–9] as well as to the discovery of new drugs.[10,11]

The main bottleneck for the successful prediction of rate constants and equilibrium constants is the accuracy in the determination of BHs and REs.[3,10] Because of the exponential dependence of these constants on the corresponding energies, an accuracy of about RT (0.6 kcal/mol at room temperature) or better is required.[12] Quantum mechanical methods based on wavefunction theory,[12–15] particularly recent composite methods, are able to calculate BHs and REs to this level of accuracy,[16–18] but they are not applicable to molecules with sizes typically encountered in organic chemistry, let alone biochemistry.[3] As a consequence of the tradeoff between accuracy and computational cost, the most popular method for thermochemical and kinetic

calculations in organic reactions is density-functional theory (DFT).[10] In reactions of biochemical interest, where the reactant molecules are much larger, DFT is typically combined with force fields in hybrid quantum mechanics/molecular mechanics (QM/MM) approaches.[6,7,19] In either case, the accuracy of the methods typically employed is often sufficient for gauging the relative energies of various mechanistic pathways but not enough to reliably predict rate constants of chemical reactions.[10,20] Consequently, the search for a standard method for kinetic and mechanistic studies is still ongoing.[4,5]

To develop new computational methods for the study of chemical reactions, and to assess the existing ones, high-quality benchmark sets are necessary.[21–27] These benchmark sets comprise REs and BHs of model reactions calculated at a very accurate level of theory, typically coupled-cluster theory (CC) with large basis sets and a complete-basis-set (CBS) extrapolation[16] (CCSD(T)/CBS is a very popular method[12]). Besides the obvious requirement that the reference data be accurate, there are a number of additional desirable traits for BH and RE benchmark sets. First, the set of reactions must be sufficiently large for the analysis to be statistically significant, and diverse enough to catch

any particularities or biases of the method under study. For instance, most DFT methods tend to underestimate BH of pericyclic reactions because the transition state (TS) is overstabilized due to delocalization error.[28,29] Second, non-covalent interactions between reactants play an important role in stabilizing the TS.[30] The importance of this stabilization increases with the size of the reactant molecules and it is particularly important in biochemical studies where, for instance, the shape of the active site determines the activity and specificity of enzymes.[4] Therefore, it is essential that the reactant molecules in the benchmark set are large enough to correctly assess the method under study regarding its ability to describe non-covalent interactions.[19,30–33]

There are difficulties with the creation of benchmark sets for BHs and REs with the aforementioned characteristics. The generation of TSs is not easily automatized.[10,20] More importantly, the computational cost involved in the calculation of accurate reference data limits the number of reactions in the set and the size of the reactant molecules. As a consequence, previously proposed benchmark sets use model reactions with small reactant molecules that are not representative of the typical reactions commonly found in mechanistic studies.[34–37] Other benchmark sets either focus on specific types of reactions, or they contain only a handful of data points, or they are not evaluated using a reference level of enough quality to allow benchmarking commonly used quantum mechanical methods.[29,32,33,38–44] The current necessity of a benchmark set for enzymatically catalyzed reactions has been emphasized several times recently.[32,33,45]

Local correlation methods, particularly DLPNO-CCSD(T), have become very popular recently due to a favorable combination of relatively high accuracy and modest computational cost.[46–51] Thanks to its near-linear-scaling nature, DLPNO-CCSD(T) can be applied to reasonably large systems.[19] Since conventional CCSD(T)/CBS is at least two orders of magnitude more accurate than the methods typically assessed with BH and RE benchmark sets, a tradeoff is used in this work. By using DLPNO-CCSD(T)/CBS for the reference energies, we designed a benchmark set (called BH9) that has the desirable features listed above, namely, the reactions in BH9 are numerous and diverse and the reactants are relatively large. The accuracy penalty in using the DLPNO approximation[31,52] is evaluated, providing an accuracy limit for the assessment of approximate methods. Variants of the DLPNO-CCSD(T)/CBS approach have been used in other recently proposed benchmark sets.[32,33,53,54]

To our knowledge, BH9 is the most comprehensive benchmark set for BHs and REs of organic and bio-organic reactions to date. Our particular objective with this set is to aid in the development of atom-centered potentials[55–57] (ACPs), whose training

requires a large and diverse set of molecular properties. However, recent machine-learning-based methods can equally benefit from using the BH9 data. Furthermore, the reference BHs and REs in BH9 can be recalculated should further developments in computational methods or computer hardware occur, without the need to find TSs for new reactions, a task that is often non-trivial.

We also present two simple applications of the new benchmark set. First, we use BH9 to assess several popular density functional approximations used in mechanistic studies. The effect of including corrections for dispersion interactions is considered, and we analyze the performance of these functionals individually for the different types of reactions included in the BH9 set. Second, the application of DFT to reaction mechanisms in practice often requires using a finite basis set due to computational constraints. Therefore, we also study the performance of our basis set incompleteness potentials[55,56] (BSIP) regarding their ability to mitigate basis set incompleteness error in the calculation of REs and BHs.

DESIGN OF BH9 AND COMPUTATIONAL DETAILS

Design of the BH9 benchmark set

The BH9 set contains 449 elementary chemical reactions, categorized in the reaction types shown in Table I. The reference data comprises the corresponding 449 REs and 898 BHs (forward and reverse), as well as the structures of reactants, products, and transition states. Table I also shows a prototype reaction for each type. The full list of diagrams for each reaction is given in the Supporting Information (SI), as well as the reference BHs, REs, and the geometries of all the molecular species. The data for each reaction is given in the form of "db" files. This plain-text file format has been described elsewhere.[58,59] A representative subset of the BH9 set can be statistically derived using, for instance, the technique described in Ref. 60.

The reaction types in Table I represent a diverse set of reactions that are common in organic and bio-organic chemistry, although the list is by no means exhaustive. Most reaction types and many of the particular reactions included in the BH9 set were adopted from the Mechanism and Catalytic Site Atlas (M-CSA) database,[61] and are known to occur in biological systems. However, some reaction types that are important in organic chemistry, such as pericyclic, hydride-transfer, and halogen-atom transfer reactions, are relatively rare in biological contexts or are not sufficiently represented in the M-CSA. For these reaction types, we explored the literature and compiled a number of reactions from various published mechanistic studies in order to

TABLE I. Reaction types in the BH9 set.

	Reaction type	Number[a]	Example reaction[b]
I	Radical rearrangement and addition	48	
II	Pericyclic	140	
III	Halogen atom transfer	43	
IV	Hydrogen atom transfer	90	
V	Hydride transfer	42	
VI	B- and Si- containing reactions	35	
VII	Proton transfer	10	
VIII	Nucleophilic substitution	15	
IX	Nucleophilic addition	26	

[a] Number of reactions in each type.
[b] Example reaction for each type.

complete our database.[62–106]

For the sake of simplicity, and due to our desire for this set to serve as a basis for ACP development, all molecules in BH9 contain exclusively elements common in organic chemistry (H, C, N, O, F, P, S, Cl). We also included a specific set of reactions containing Si and B (reaction type VI in Table I). The fact that there are no transition metals in the BH9 reactions simplifies the application and interpretation of the tests based on this set, particularly regarding the application of BH9 to the assessment of DFT methods. RE and BH benchmark sets for reactions containing transition metals have been proposed recently,[53,54,107,108] some of them also at DLPNO-CCSD(T) level.[53,54] The sizes of the reactant and TS molecules in BH9 range from 11 to 71 atoms—significantly larger than most previous sets, and typical of mechanistic studies.

Some of the reactions in BH9, particularly nucleophilic

substitutions, nucleophilic additions, and proton transfer reactions, involve charged species. In this case, we expect the species involved in the reaction, and particularly reactants and products, to be greatly stabilized by interactions with the solvent or the environment. We experienced difficulties finding some of these TSs, which is why the number of reactions in these three categories is smaller than the others (see Table I). In addition, some of the BHs are negative, possibly because the solvent stabilizes reactants and products more than it stabilizes the TS. Although we eliminated very negative BHs from the set, some were left for the sake of diversity. A similar decision was taken by Iron et al. for their BH set for reactions involving transition metals.[53]

Location of the transition states, reactant and product structures

Guess TSs were built for the 449 reactions in the BH9 set. This was a laborious process because of the difficulty in locating TSs with the currently available algorithms in standard software packages. In addition to not being automatic, the TS search often failed entirely, which explains the uneven number of reactions in each category of Table I. Because of their relatively large size and the abundance of reactions, reliably locating the minimum-energy conformer for each species in the BH9 is a formidable problem. However, in order for the BHs to still be representative of the corresponding reactions, we devised a protocol that explores the conformational landscape of reactants, products, and TS. This protocol, described in the SI, ensures that the proposed structures are reasonably close in energy, if not identical, to the global energy minima of all species.

The initial reactant and product structures were constructed from the optimized TS structures and subjected to geometry optimizations followed by conformer exploration, in a manner similar to the TS structure search. More details can be found in the SI.

Reference energy calculations

The reference BHs and REs were obtained using single-point DLPNO-CCSD(T)[46–51] (in particular, DLPNO-CCSD(T0)) at the equilibrium geometries of reactants, products, and TSs. The favorable scaling of DLPNO-CCSD(T) makes it possible to apply CC to the fairly large molecules included in BH9, which is why this method has been often used to generate reference data in recent benchmark sets.[32,53,54] Naturally, the use of the DLPNO approximation introduces an error compared to canonical CCSD(T). The reference energies are calculated using a focal-point approach to minimize the computational cost associated with using large basis sets.[12] The error introduced by DLPNO as well as the convergence of the reference data with respect to basis set size are examined in the Results and Discussion section. More details regarding the reference energy calculations can be found in the SI.

DFT calculation details

DFT calculations were used to assess the performance of various density functional approximations commonly used in mechanistic studies[10] on the BH9 set. The list of functionals surveyed includes semilocal (BLYP,[109,110] PBE,[111] TPSS,[112] revTPSS,[113] MN15-L,[114] and B97M-V[115]), global (B3LYP,[110,116] PBE0,[117] BH&HLYP,[110,118] M05-2X,[119] M06-2X,[120] and

MN15[121]), and range-separated hybrid functionals (CAM-B3LYP,[122] LC-ωPBE,[123,124] ωB97XD,[125,126] ωB97M-V,[127] and ωB97X-V[128]). Further computational details can be found in the SI.

To evaluate the importance of dispersion, the exchange-hole dipole moment (XDM) model was used in combination with some of the functionals above.[129,130] The canonical complete-basis-set XDM damping function parameters and the postg program were used.[131,132] We expect the conclusions from this analysis to be transferable to other dispersion corrections, such as Grimme's Dn family.[133]

Due to the typical size of the molecular species involved, the availability of computationally inexpensive methods for thermochemistry and kinetics is very important in the study of biochemical reactions.[57] One of the major factors impacting the accuracy of DFT methods in this context is BSIE, which arises from the finite nature of the basis sets employed. For this reason, we also examine the performance of our recently proposed basis set incompleteness potentials[56] (BSIPs) combined with several double-ζ basis sets in the description of REs and BHs. In particular, we evaluated the PBE0-XDM functional[117,130] combined with the BSIP-corrected 6-31G∗, 6-31+G∗, 6-31+G∗∗,[134–136] Def2-SV(P), Def2-SVP,[137] and pc-1 basis sets.[138–141]

RESULTS AND DISCUSSION

Evaluation of the reference data

The most popular calculation level for benchmark sets is CCSD(T) with CBS extrapolation, which is known to yield sub-kcal/mol accuracy.[12,142] As mentioned above, this level of theory is too computationally demanding and cannot be used to generate reference data for BH9, so we opted for DLPNO-CCSD(T) instead. We expect the two primary sources of error are our choice of basis set extrapolation strategy[12] and the application of the DLPNO approximation.[31] In this section, we evaluate the importance of both sources of error and we provide a reasonable estimate for the error bars associated with the BH9 reference data. Ultimately, this error estimate constitutes the accuracy limit of the BH9 set; methods more accurate than those applied here cannot be reliably assessed with this set.

The reference data was calculated using the focal-point approach[143,144] described in the SI. To estimate the overall error in the BH9 reference data and to assess each of the approximations made, we selected a small subset of BH9 containing 17 reactions with relatively small molecules. This subset is shown in Table II. Since errors in the calculation of REs are typically lower than BHs,[31] we focus on the latter. The small size of the molecules in this subset allows the calculation of

TABLE II. Subset of the BH9 reactions used for assessing the quality of the reference data.

	Reaction	Type
1		Radical rearrangement (I)
2		Radical rearrangement (I)
3		Radical rearrangement (I)
4		Pericyclic (II)
5	[3+2]	Pericyclic (II)
6	Electrocyclic	Pericyclic (II)
7	Electrocyclic	Pericyclic (II)
8	[3,3]-Claisen	Pericyclic (II)
9		Hydrogen atom transfer (IV)
10		Hydrogen atom transfer (IV)
11		Si-containing (VI)
12		Si-containing (VI)
13		Proton transfer (VII)
14		Proton transfer (VII)
15		Nucleophilic substitution (VIII)
16		Nucleophilic substitution (VIII)
17		Nucleophilic addition (IX)

TABLE III. Barrier heights for the reactions in Table II calculated using various levels of theory.[a]

Reaction[g]	HF					ΔMP2[f]					ΔCCSD(T)[f]		CCSD(T)	
	aTZ[b]	aQZ[b]	a5Z[b]	a{T,Q}Z[c]	a{Q,5}Z[c]	aTZ[b]	aQZ[b]	a5Z[b]	a{T,Q}Z[c]	a{Q,5}Z[c]	DLPNO aTZ[b]	Can.[d] aTZ[b]	DLPNO CBS[e]	Can.[d] CBS[e]
1 F	16.84	16.85	16.85	16.85	16.85	−1.25	−1.08	−1.27	−0.96	−1.47	−4.15	−3.76	11.74	12.13
1 R	10.09	10.15	10.15	10.17	10.14	5.30	5.46	5.58	5.57	5.71	−6.74	−6.35	9.01	9.39
2 F	16.38	16.42	16.44	16.43	16.44	4.80	5.13	5.24	5.36	5.36	−1100	−1080	10.80	11.00
2 R	26.39	26.42	26.41	26.43	26.41	−4.18	−4.03	−3.96	−3.92	−3.90	−1.98	−1.69	20.54	20.82
3 F	15.67	15.84	15.86	15.89	15.86	−0.96	−0.68	−0.55	−0.48	−0.42	−6.85	−6.78	8.56	8.63
3 R	19.79	19.70	19.69	19.67	19.69	−6.12	−6.01	−5.98	−5.93	−5.94	−2.90	−2.62	10.84	11.13
4 F	42.42	43.16	43.46	43.36	43.51	−3938	−3845	−3806	−3778	−3765	11.41	10.46	16.98	16.03
4 R	70.71	70.48	70.29	70.41	70.26	−1548	−1546	−1539	−1544	−1532	4.49	3.74	59.46	58.71
5 F	41.06	41.34	41.45	41.41	41.47	−3595	−3532	−3519	−3487	−3506	8.89	8.02	15.43	14.56
5 R	87.78	87.91	87.88	87.95	87.88	−3215	−3160	−3134	−3121	−3106	11.55	10.69	68.29	67.44
6 F	41.85	41.97	41.97	42.00	41.97	−1106	−1093	−1082	−1083	−1071	1.91	1.62	33.08	32.78
6 R	59.96	60.12	60.15	60.16	60.15	−1888	−1866	−1861	−1850	−1855	3.76	3.58	45.42	45.24
7 F	56.32	56.42	56.43	56.45	56.43	−1428	−1395	−1381	−1372	−1366	1.55	1.12	44.28	43.84
7 R	70.99	71.10	71.15	71.13	71.15	−2069	−2034	−2025	−2008	−2016	3.30	3.01	54.35	54.06
8 F	50.55	50.77	50.83	50.83	50.84	−2591	−2553	−2541	−2527	−2529	6.51	5.68	32.08	31.25
8 R	69.02	69.36	69.39	69.44	69.40	−2553	−2543	−2530	−2536	−2516	5.53	4.62	49.61	48.70
9 F	28.85	29.05	29.08	29.11	29.09	−9.04	−8.73	−8.60	−8.51	−8.48	−4.18	−4.47	16.42	16.13
9 R	33.81	33.93	33.96	33.96	33.96	−2261	−2281	−2280	−2295	−2280	1.36	1.06	12.36	12.06
10 F	21.25	21.42	21.55	21.47	21.57	−1687	−1683	−1682	−1681	−1681	0.13	−0.36	4.80	4.30
10 R	21.34	21.51	21.63	21.55	21.65	−1717	−1710	−1708	−1705	−1706	0.08	−0.25	4.58	4.25
11 F	34.65	35.21	35.38	35.36	35.41	−2200	−2202	−2191	−2204	−2179	2.40	1.44	15.72	14.76
11 R	19.87	19.85	19.78	19.84	19.77	−4.60	−4.32	−4.16	−4.12	−3.98	−5.04	−5.70	10.68	10.02
12 F	8.54	8.64	8.66	8.66	8.66	−2.00	−1.60	−1.48	−1.32	−1.36	−5.11	−5.10	2.24	2.25
12 R	30.06	30.47	30.72	30.57	30.76	3.11	3.41	3.57	3.62	3.74	−5.84	−5.80	28.35	28.39
13 F	49.98	50.22	50.24	50.28	50.25	−1590	−1608	−1611	−1620	−1614	3.21	2.93	37.29	37.01
13 R	51.08	51.28	51.31	51.33	51.32	−1450	−1464	−1469	−1475	−1475	1.62	1.37	38.20	37.96
14 F	2.70	2.76	2.77	2.78	2.77	−2.24	−2.19	−2.16	−2.16	−2.12	0.22	0.26	0.84	0.87
14 R	2.96	3.03	3.05	3.05	3.05	−2.95	−2.99	−2.96	−3.02	−2.93	0.72	0.75	0.75	0.78
15 F	3.80	3.93	3.99	3.97	4.00	−6.03	−5.94	−5.77	−5.88	−5.60	−1.29	−1.88	−3.21	−3.80
15 R	25.57	25.87	26.01	25.95	26.03	−1134	−1127	−1123	−1123	−1118	0.34	−0.34	15.07	14.39
16 F	25.57	25.71	25.73	25.75	25.73	−1153	−1124	−1120	−1104	−1115	−0.42	−1.09	14.28	13.62
16 R	2.72	3.28	3.63	3.43	3.68	−1.87	−1.90	−1.92	−1.91	−1.95	−1.56	−2.12	−0.05	−0.61
17 F	13.08	13.40	13.43	13.48	13.44	−1669	−1660	−1642	−1654	−1622	2.11	1.68	−0.94	−1.38
17 R	3.48	3.39	3.39	3.36	3.39	2.93	3.02	3.02	3.09	3.01	−1.64	−1.68	4.81	4.77
MAE	0.27	0.08	0.01	0.05		0.42	0.21	0.11	0.11		0.43		0.43	

[a] Units are kcal/mol. [b] aNZ = aug-cc-pVNZ basis set. [c] a{X,Y}Z = two-point HF or correlation energy extrapolation as described in the text. [d] Can. = canonical. [e] CBS = complete-basis-set extrapolation (Eq. ??). [f] ΔMP2 = $E_{\mathrm{MP2}} - E_{\mathrm{HF}}$. ΔCCSD(T) = $E_{\mathrm{CCSD(T)}} - E_{\mathrm{MP2}}$. [g] F = forward reaction, R = reverse reaction.

canonical CCSD(T)/aTZ energies, as well as HF/a5Z and MP2/a5Z. These last two quantities permit the calculation of the extrapolated aQZ/a5Z HF and MP2 barrier heights. For the MP2 correlation energy, we used the same two-point extrapolation formula (Eq. 5 in the SI) with the asymptotic value $\beta = 3$.[145,146] For the HF energy, we used the extrapolation formula proposed by Karton and Martin for this particular basis set pair.[147,148]

The BHs obtained with these methods are shown in Table III. We first consider the impact of basis set incompleteness on the individual components of our reference BHs. In the case of HF, our best CBS estimate (a{Q,5}Z extrapolation) agrees with HF/a5Z to within 0.01 kcal/mol on average, indicating that both are converged to within this value. Our chosen reference method for the HF component (a{T,Q}Z extrapolation) has a mean absolute error (MAE) of only 0.05 kcal/mol with respect to the aQZ/a5Z result. The highest deviations happen for reactions involving second-row atoms: numbers 6 (0.10 kcal/mol, both directions), 4 (0.15 kcal/mol, both directions), 8 (0.19 kcal/mol, reverse), and 12 (0.25 kcal/mol, reverse).

As noted above, the MP2 correlation energy converges more slowly to the CBS than the HF energy so, as expected, the basis set incompleteness errors are higher. The MP2 correlation contribution used in our reference method (a{T,Q}Z extrapolation) has the same MAE as MP2/a5Z (0.11 kcal/mol) compared to our best MP2/CBS estimate (a{Q,5}Z extrapolation). In this case, the large errors are not associated with second-row atoms, and they can be as high as half a kcal/mol (0.51 kcal/mol for forward reaction 1 and 0.32 kcal/mol for forward reaction 13). Combining the HF and MP2 results, we expect the average error from the HF+MP2 contribution to be in the vicinity of 0.2 kcal/mol, with worst cases being between 0.5 and 1 kcal/mol. Due to computational constraints, we cannot estimate the error introduced by calculating $\Delta E_{\text{CCSD(T)}}$ at aTZ level, although past experience with non-covalent interactions suggests that it is in the range of tenths of a kcal/mol or lower.[149]

The last four columns in Table III show the error introduced by the DLPNO approximation by comparing the $\Delta E_{\text{CCSD(T)}}$ contribution and the total BH with and without DLPNO. The MAE from the DLPNO approximation is 0.43 kcal/mol, which is very similar to the 0.51 kcal/mol reported by Paiva et al. for enzymatic reactions.[52] However, there are a few reactions where the deviations between DLPNO and canonical CCSD(T) are significantly higher, although lower than 1 kcal/mol in all cases: reactions 17 (0.83 kcal/mol and 0.91 kcal/mol), 14 (0.86 and 0.87 kcal/mol), and 4 (0.95 and 0.75 kcal/mol). The reactions for which the maximum deviation is observed are all pericyclic reactions, which agrees with the recent report by

Sandler et al. who showed that DLPNO error is higher for dispersion-dominated and Diels-Alder BHs, with errors that can be as high as 1.2 kcal/mol.[31] The behavior of the errors in Table III confirm the relative difficulty of the DLPNO approximation in modeling large dispersion-dominated systems: All bimolecular BHs are overestimated, and the error for the forward and reverse reactions is approximately the same, indicating that the TSs are predicted to be too unstable by DLPNO. Based on these observations and the fact that the reaction subset in Table II contains the smallest molecules in BH9, we expect the 0.43 kcal/mol to be an overly optimistic error bar. An average error from the DLPNO approximation of around 0.5–1 kcal/mol for the reference data in BH9 is probably a more realistic estimate.

On the grounds of the preceding analysis, it is clear that the DLPNO approximation is the main contributing factor to the error in the BH9 reference data. Since basis set incompleteness is not the leading contribution to the error, our basis set extrapolation approach is justified.[150] Our analysis also shows that the estimated error is low enough to benchmark density functional approximations, which have typical errors in the range of a few kcal/mol[22] (see below). The reference data can be revised in the future as more powerful computers and better algorithms become available.

Assessment of density functional theory methods

We now proceed to assess a few density functionals that are popular in mechanistic studies with the BH9 set. Our objectives are: i) evaluate whether the increased number of reactions and the larger molecules in the BH9 offer a picture of the performance of these functionals for thermochemistry and kinetics that is different from previous studies,[21,22,130,151] ii) analyze the errors in the BH and RE calculations as a function of reaction type, and iii) benchmark the available XDM-corrected density functionals regarding their ability to calculate REs and BHs, something that has been done previously only with a very limited set of reactions.[130] We expect the inclusion of XDM dispersion to have a similar effect to D3, which has been extensively studied.[22,151]

Tables IV and V show the mean absolute error (MAE) and mean error (ME) of the selected functionals for REs and BHs, grouped by type. The overall RE and BH MAEs are shown graphically in Figure 1. In agreement with previous studies,[22,130,151] the performance of hybrid and range-separated hybrid functionals is, in general, much better than that of GGA functionals. The best-performing functional is ωB97M-V, with 1.68 kcal/mol MAE for reaction energies and 2.08 kcal/mol MAE for barrier heights. The best-performing semilocal (meta-GGA) functional is MN15-L with MAEs of 3.99 kcal/mol for barrier heights

TABLE IV. Average errors in the BH9 reaction energies using various density functionals.[a]

Functional		I	II	III	IV	V	VI	VII	VIII	IX	Total
BLYP	MAE	8.42	22.27	8.75	3.17	2.35	11.70	2.82	4.01	10.84	11.27
	ME	8.42	20.96	−176	−124	0.01	10.59	0.87	−078	10.84	8.47
BLYP-XDM	MAE	5.27	13.87	7.77	2.77	2.24	3.92	2.70	3.50	4.65	7.15
	ME	5.24	12.51	−109	−117	−002	3.11	0.64	−087	4.56	4.61
PBE	MAE	3.34	10.52	8.71	3.24	2.49	5.79	3.00	4.04	3.67	6.22
	ME	1.56	9.36	−195	−102	1.52	4.78	0.50	−129	2.44	3.32
PBE-XDM	MAE	2.68	7.59	8.36	3.12	2.48	2.26	3.00	4.00	3.14	4.87
	ME	0.68	6.36	−172	−101	1.49	1.36	0.44	−143	0.02	1.90
TPSS	MAE	4.10	13.81	8.34	3.14	2.45	8.22	2.48	3.72	5.57	7.54
	ME	2.96	12.84	−156	−088	1.24	7.12	0.66	−124	5.49	4.95
TPSS-XDM	MAE	2.82	8.87	7.73	2.94	2.51	3.01	2.44	3.13	2.87	5.19
	ME	1.26	7.79	−116	−085	1.24	2.10	0.54	−137	1.64	2.62
revTPSS	MAE	3.32	10.91	7.82	3.37	2.82	7.46	2.12	3.76	3.95	6.43
	ME	1.22	9.92	−120	−076	1.58	6.48	0.64	−136	3.76	3.80
MN15-L	MAE	2.16	5.72	6.36	2.36	4.04	2.60	2.63	2.75	2.75	3.99
	ME	−004	4.57	−070	−098	−298	−029	0.11	−118	0.88	0.87
B97M-V	MAE	2.18	6.66	6.44	2.49	2.92	2.32	2.09	2.62	2.48	4.15
	ME	0.70	5.50	−073	−092	−203	0.84	0.27	−057	0.74	1.44
B3LYP	MAE	5.63	15.65	7.12	2.40	2.56	8.91	1.81	2.77	8.02	8.18
	ME	5.62	14.75	−047	−091	−167	7.94	0.61	−028	8.02	5.90
B3LYP-XDM	MAE	3.69	9.85	6.37	2.06	2.45	2.78	1.76	2.16	3.68	5.26
	ME	3.62	8.89	−000	−087	−169	2.20	0.47	−044	3.49	3.20
PBE0	MAE	2.69	5.52	6.25	2.19	1.73	4.14	1.77	2.57	2.12	3.78
	ME	−081	3.91	−105	−046	−050	3.18	0.23	−059	0.92	1.18
PBE0-XDM	MAE	2.40	3.18	5.89	2.02	1.63	1.39	1.77	2.22	2.49	2.74
	ME	−167	0.95	−083	−046	−052	−022	0.17	−072	−148	−022
BH&HLYP	MAE	3.46	9.42	4.80	1.60	4.11	6.31	0.87	2.07	5.44	5.37
	ME	3.32	8.78	0.14	−031	−302	5.42	0.45	0.66	5.42	3.53
BH&HLYP-XDM	MAE	2.22	5.36	4.33	1.33	3.97	2.39	0.86	1.43	2.39	3.36
	ME	2.01	4.58	0.46	−032	−301	0.95	0.36	0.53	2.10	1.57
M05-2X	MAE	1.61	3.12	4.55	1.26	2.54	1.73	0.92	1.83	1.69	2.39
	ME	0.28	2.30	1.10	−043	−165	0.89	−008	0.03	0.75	0.72
M06-2X	MAE	2.31	4.00	4.72	1.56	1.47	2.36	0.91	1.84	1.71	2.76
	ME	0.51	3.71	0.80	−063	−058	1.76	−014	−056	1.36	1.30
MN15	MAE	1.94	4.14	6.07	1.94	4.19	2.22	1.86	2.03	1.77	3.25
	ME	−020	3.26	−001	−078	−303	1.03	−012	−068	1.19	0.68
CAM-B3LYP	MAE	2.98	8.37	5.29	1.62	2.62	5.89	1.08	1.82	4.67	4.82
	ME	2.72	7.83	−029	−052	−160	5.10	0.57	0.07	4.65	3.13
CAM-B3LYP-XDM	MAE	2.10	5.03	4.87	1.43	2.57	2.11	1.08	1.30	2.14	3.14
	ME	1.71	4.42	−002	−051	−164	1.19	0.50	−012	1.80	1.51
LC-ωPBE	MAE	4.28	4.38	5.90	1.66	1.73	2.98	1.19	1.82	1.72	3.30
	ME	−368	−257	0.11	−018	1.00	1.68	0.76	0.20	0.01	−097
LC-ωPBE-XDM	MAE	4.83	6.84	5.54	1.63	1.69	2.99	1.18	1.50	2.62	4.13
	ME	−483	−618	0.39	−016	1.13	−204	0.69	0.21	−257	−262
ωB97XD	MAE	1.76	3.03	5.27	1.71	1.32	1.94	1.34	1.19	1.69	2.42
	ME	0.08	2.04	−008	−048	−011	−042	0.49	−022	1.24	0.57
ωB97X-V	MAE	2.12	2.39	5.09	1.74	1.05	2.24	1.00	1.20	1.37	2.22
	ME	−185	−188	0.37	−032	0.06	−089	0.52	0.02	−106	−093
ωB97M-V	MAE	1.28	1.36	4.20	1.43	1.73	1.94	0.89	1.37	0.99	1.68
	ME	−026	0.56	0.28	−058	−088	−046	0.09	−007	0.29	−005

[a] Units are kcal/mol. MAE = mean absolute error. ME = mean error. The roman numerals represent the reaction types in Table II.

and 3.57 kcal/mol for reaction energies. Also, Figure 1 shows that there is a degree of positive correlation between RE and BH average errors, indicating that functionals that perform well for REs tend to work for BHs as well.

Compare to the best-performing functional (ωB97M-v), ωB97XD, M05-2X, M06-2X, and MN15 functionals have similar performance for the barrier heights (in the 2–2.5 kcal/mol range), but differ for reaction energies with MAEs between 2.39 kcal/mol

TABLE V. Average errors in the BH9 barrier heights using various density functionals.[a]

Functional		I	II	III	IV	V	VI	VII	VIII	IX	Total
BLYP	MAE	5.01	12.19	7.54	4.87	5.05	7.35	3.40	4.00	5.73	7.62
	ME	−377	−594	−646	−197	0.29	2.74	−156	−209	−345	−333
BLYP-XDM	MAE	5.05	10.26	11.86	8.51	10.67	4.45	3.62	8.72	6.16	8.66
	ME	−505	−107	−186	−849	−142	−306	−353	−872	−589	−844
PBE	MAE	3.85	7.98	8.59	7.01	7.59	3.99	5.51	4.04	4.77	6.68
	ME	−369	−655	−848	−662	−657	−146	−486	−327	−451	−578
PBE-XDM	MAE	4.18	8.20	10.99	9.63	12.04	4.39	5.65	6.32	5.57	8.12
	ME	−418	−816	−109	−960	−196	−429	−564	−629	−544	−807
TPSS	MAE	3.89	9.04	6.88	4.84	4.78	5.23	3.84	4.04	4.44	6.19
	ME	−352	−641	−638	−308	−181	−010	−263	−313	−385	−417
TPSS-XDM	MAE	4.33	9.07	10.04	7.56	9.66	4.30	3.97	7.57	5.47	7.66
	ME	−433	−905	−104	−752	−947	−413	−385	−757	−536	−761
revTPSS	MAE	3.86	8.12	6.99	4.53	4.43	5.03	3.14	4.08	4.19	5.78
	ME	−365	−654	−666	−292	−206	−113	−183	−344	−385	−431
MN15-L	MAE	1.50	3.88	4.54	3.79	6.01	2.53	3.07	2.42	1.71	3.57
	ME	−021	−240	−209	−280	−576	−203	1.35	0.45	−072	−223
B97M-V	MAE	1.75	4.28	6.38	4.52	7.13	1.97	1.67	2.88	2.47	4.14
	ME	−149	−345	−605	−440	−696	−112	−043	−252	−214	−365
B3LYP	MAE	2.98	8.08	4.27	3.66	5.69	5.88	1.75	3.58	4.10	5.37
	ME	−104	−089	−108	1.08	4.81	4.23	0.11	2.02	−095	0.52
B3LYP-XDM	MAE	2.34	5.51	5.81	4.03	4.05	2.43	1.58	3.09	3.13	4.22
	ME	−197	−391	−517	−395	−373	−033	−128	−299	−268	−338
PBE0	MAE	1.46	3.34	3.47	3.08	3.82	2.72	2.76	3.85	1.62	3.00
	ME	−028	−005	−076	−095	1.53	1.56	−191	2.93	−101	−005
PBE0-XDM	MAE	1.43	2.54	3.87	3.98	4.09	1.55	2.76	1.52	2.13	2.85
	ME	−077	−166	−325	−391	−389	−128	−269	−006	−193	−233
BH&HLYP	MAE	2.55	7.27	7.54	6.82	14.49	7.21	3.36	7.03	3.39	7.05
	ME	2.25	6.68	6.69	6.81	14.49	7.18	3.36	6.98	3.07	6.73
BH&HLYP-XDM	MAE	1.81	4.92	4.43	2.99	7.50	3.71	2.30	3.22	1.96	4.01
	ME	1.55	4.41	3.45	2.85	7.48	3.52	2.30	3.06	1.77	3.67
M05-2X	MAE	0.96	1.94	2.90	1.56	6.30	1.72	1.26	2.97	1.06	2.21
	ME	0.03	0.15	1.38	0.36	5.70	0.53	−032	2.25	−057	0.86
M06-2X	MAE	1.61	2.39	2.96	1.36	4.99	1.66	1.11	3.14	1.13	2.27
	ME	1.06	0.92	2.03	−030	4.44	0.37	−022	2.76	−028	1.05
MN15	MAE	1.09	2.34	3.63	1.90	3.17	1.53	1.52	2.75	1.07	2.18
	ME	0.37	0.11	1.90	0.14	1.83	−083	−038	2.11	−002	0.45
CAM-B3LYP	MAE	1.83	5.06	4.18	3.20	9.34	5.21	1.21	4.89	2.41	4.43
	ME	1.19	3.86	2.28	2.47	9.05	5.05	0.16	4.65	1.29	3.52
CAM-B3LYP-XDM	MAE	1.27	3.16	2.55	1.68	3.50	2.26	1.07	2.13	1.19	2.37
	ME	0.63	2.03	−046	−086	3.13	1.85	−070	1.31	0.25	0.96
LC-ωPBE	MAE	3.70	9.15	8.47	4.82	13.79	5.38	1.40	10.38	3.70	7.33
	ME	3.49	9.12	8.31	4.66	13.37	5.18	0.13	10.38	3.63	7.16
LC-ωPBE-XDM	MAE	3.16	7.15	5.59	1.52	7.35	2.60	1.22	6.87	2.84	4.72
	ME	2.88	7.13	5.32	1.12	6.86	2.09	−089	6.87	2.46	4.42
ωB97XD	MAE	1.13	2.66	2.97	1.73	2.17	1.58	0.90	2.99	1.21	2.10
	ME	0.65	2.26	1.91	−120	1.46	0.80	0.04	2.79	0.58	1.04
ωB97X-V	MAE	1.69	4.57	3.69	1.24	6.36	2.02	0.70	3.71	1.70	3.20
	ME	1.46	4.57	2.52	−010	6.08	1.65	0.01	3.51	1.51	2.70
ωB97M-V	MAE	1.00	2.15	2.56	1.11	6.16	1.40	0.68	2.20	0.99	2.08
	ME	0.81	2.06	0.50	0.09	5.65	0.34	0.07	1.67	0.58	1.45

[a] Units are kcal/mol. MAE = mean absolute error. ME = mean error. The roman numerals represent the reaction types in Table II.

(M05-2X) and 3.25 kcal/mol (MN15). The ωB97X-V functional is reasonably accurate for reaction energies (MAE = 2.22 kcal/mol) but not for barrier heights (MAE = 3.20 kcal/mol) compared to the rest. The good performance of these functionals (or variants of ωB97X in combination with other dispersion corrections) has been noted in previous works.[21,22,53] Close in performance are also PBE0-XDM (MAE(RE) = 2.74 kcal/mol; MAE(BH) = 2.85 kcal/mol) and CAM-B3LYP-XDM (MAE(RE) = 3.14 kcal/mol; MAE(BH) = 2.37 kcal/mol). B3LYP

FIG. 1. Barrier height vs. reaction energy mean absolute errors (MAE) for the chosen functionals. Open symbols represent the XDM-corrected version of each functional.
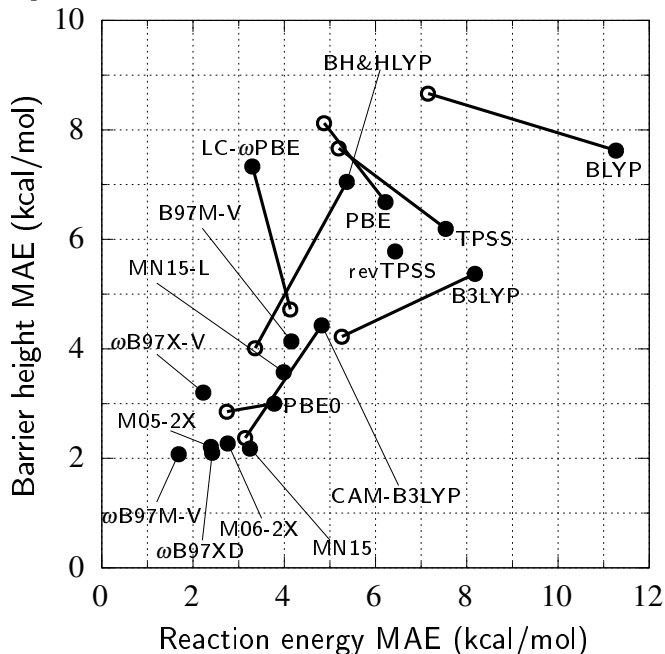
performs relatively poorly both in RE and BH, and so does its XDM-corrected version with average errors slightly over 4 kcal/mol.

The good performance of M05-2X and M06-2X is interesting. It is known that these functionals underestimate non-covalent interaction energies at long range.[152,153] Since the importance of long-range dispersion increases with molecular size,[154] one would have expected a degradation in the performance of these functionals for the BH9 relative to previous studies of REs and BHs involving smaller molecules.[22,152] However, this does not seem to be the case, and our average errors are similar to those reported by Mardirossian et al.[152] and Goerigk et al.[22] Because TSs of addition reactions are larger than either the reactant or product molecules, an underestimation of non-covalent binding would lead to an erroneously unstable TS and an overestimation of the BHs. This seems to be the case for M05-2X and M06-2X, as indicated by the MEs in Table V. However, the average bias is only 0.72 (M05-2X) and 1.30 kcal/mol (M06-2X) for REs and 0.86 (M05-2X) and 1.05 kcal/mol (M06-2X) for BHs, suggesting that capturing the correct asymptotic dependence of the dispersion contribution seems not to be as important for the calculation of REs and BHs as previously argued.[22] This point is reinforced by the fact that the performance of M05-2X and M06-2X in the GMTKN database is only marginally improved by their combination with the D3 dispersion correction.[22,151] It is also interesting to note that, according to their performance on the BH9, more

recent Minnesota functionals seem to perform worse than older versions. In particular, MN15 is worse for reaction energies than M05-2X or M06-2x by about 1 kcal/mol (see Figure 1).

Compared to our previous analysis of the performance of XDM-corrected functionals for REs and BHs,[130] the advantages of a more complete benchmark set are evident. In our previous work, LC-ωPBE-XDM (MAE = 1.43 kcal/mol) and BH&HLYP-XDM (MAE = 2.38 kcal/mol) were the best-performing functionals for BHs.[130] This is in stark contrast with the results in Table V and Figure 1, where the MAEs of these functionals rise to 4.72 and 4.01 kcal/mol, respectively. The cause of this disagreement is very likely the limited size of the benchmark set used in our previous work,[130] the small size of the molecular species, and the fact that it contained only hydrogen atom transfer reactions. Still, the results in Table IV, Table V, and Figure 1 are encouraging and suggest that expanding the list of functionals with which XDM has been combined could increase the applicability of the method to chemical problems other than modeling non-covalent interactions.

As expected, the effect of including the XDM dispersion energy agrees, in general terms, with previous reports in the literature using D3.[22,30,151,155,156] The inclusion of XDM has a noticeable impact on REs and BHs. Uncorrected GGAs severely overestimate REs, with an MAE that can be as high as 11.27 kcal/mol (BLYP). The overestimation is less pronounced for uncorrected hybrid and range-separated hybrid functionals. The inclusion of XDM dispersion partially corrects the overestimation of the REs and reduces the MAEs by several kcal/mol in general, except in the case of LC-ωPBE. These observations can be explained by the fact that the overall RE error is dominated by addition reactions, where the product molecule is the combination of both reactants. Functionals without dispersion underestimate the stability of the addition products, resulting in erroneously high REs.

In the case of BHs, Figure 1 and Table V show that the MAEs for the uncorrected functionals are in the range 4–8 kcal/mol. In particular, all GGA and meta-GGA functionals severely underestimate the BHs. This is explained by delocalization error,[28] the tendency of approximate density functionals to overstabilize delocalized molecules. The TS are, in general, more delocalized than reactants and products. Consequently, they are spuriously stabilized, resulting in an erroneously low BH.[28] Delocalization error severely affects GGAs, while admixture of exact exchange in global and range-separated hybrids mitigates, but does not eliminate, this problem. The effect of including the XDM dispersion energy on BHs can be understood as well. The dispersion stabilization increases with the size of the molecule, so including the dispersion energy

always leads to lower BHs. For GGAs functionals, which spuriously underestimate BHs, inclusion of XDM results in an increased MAE. For hybrid and range-separated hybrid functionals, which do not suffer as much from delocalization error, the use of XDM decreases the MAEs. This is consistent with previous analysis in the literature.[28,130,151]

We now analyze the performance of the chosen functionals on the various reaction types of the BH9 set using the data in Tables IV and V. For a few representative functionals, the RE and BH MAEs as a function of reaction type are shown in Figure 2. In the case of the REs, there are large differences between reaction types regarding the performance of various functionals and the effect of dispersion. Reaction types IV (hydrogen atom transfer), V (hydride transfer), VII (proton transfer), and VIII (nucleophilic substitution) seem to be modelable with approximately the same error by all uncorrected and dispersion-corrected functionals, in the range 2–4 kcal/mol. However, hybrid and range-separated hybrid functionals are, again, slightly better than GGAs. Reactions I (mostly radical rearrangements) and III (halogen atom transfer) show higher errors (up to around 8 kcal/mol for BLYP), are better modeled by hybrid or range-separated functionals, and the inclusion of dispersion corrections has a relatively minor impact. Reaction types VI (B- and Si-containing reactions) and IX (nucleophilic addition) show similar or larger errors than I and III and hybrid and range-separated hybrid functionals outperform GGAs. However, in this case, the inclusion of dispersion interactions improves the functional performance by several kcal/mol. These observations are easily explained by the fact that types VI and IX comprise addition reactions, while the other reaction types mentioned are rearrangements or atom transfer reactions. Since dispersion interactions stabilize larger molecules, their inclusion alleviates the overestimation of the REs in these reactions by the uncorrected functionals, as mentioned above. (Note that most REs for addition reactions are negative. Uncorrected functionals yield overestimated REs in general; their REs are above this negative reference value, but smaller in magnitude.) Lastly, the pericyclic reactions (II) show the highest errors, possibly due to the effect of varying delocalization between reactants and products, and benefit from dispersion for the same reason as VI and IX, since most of the members of this category are addition reactions.

Figure 2 and Table V show that the MAEs for BHs are higher than for REs, and that the inclusion of dispersion has comparatively more impact. BHs are more accurately represented by hybrid functionals, particularly if they are dispersion corrected, than by GGA functionals for all reaction types. For types I (radical rearrangement) and VII (proton transfer), the effect of including dispersion is minimal, and the

accuracy is entirely controlled by the base functional, with hybrid and range-separated hybrid functionals showing much better performance. In reactions II (pericyclic) and VI (B- and Si-containing reactions), including dispersion interactions either has no effect or is beneficial, regardless of the functional type. Figure 2 also shows the MAE for the forward and reverse BHs separately. Reactions II and VI are particular in that the effect of dispersion is very noticeable in the forward reaction BHs, but it is not for the reverse reaction BHs. This is reasonable because both categories comprise addition reactions. The dispersion stabilization of the product is essentially the same as the TS, but higher than for the reactant molecules. For the rest of the reactions, the inclusion of dispersion increases the MAE of the GGA functionals and decreases (in general) the MAEs of hybrid and range-separated hybrid functionals, for the reasons stated above.

The fact that the inclusion of dispersion interactions decreases the MAE for (forward) BHs in pericyclic reactions (II) is slightly surprising in light of our previous discussion regarding delocalization error. Given the delocalized nature of the TS in pericyclic reactions, we expected a severe underestimation of the forward BH by GGAs and a subsequent increase in the MAE upon application of XDM. We can interpret this by noting that the reacting molecules are larger in the pericyclic reactions than in other reactions of the BH9 set, which suggests that non-covalent interactions have a comparatively more important role in the stabilization of the TS than electronic delocalization. Omitting dispersion interactions from the functional destabilizes the TS more than the spurious stabilizing effect from delocalization error, and therefore the inclusion of XDM is beneficial.

In summary, our analysis shows that, in agreement with previous studies,[21,22] the performance of density functional approximations improves with sophistication: GGA and meta-GGA functionals are not usable in general for RE and BH prediction while hybrid and range-separated hybrid functionals offer smaller average errors. The best performer among the functionals studied is ωB97M-V, followed by the other members of the same family, the Minnesota functionals, and PBE-XDM and CAM-B3LYP-XDM. This agrees with previous works,[21,22] where these functionals, or variants of them, were shown to be among the best functionals available for the calculation of REs and BHs, except for double-hybrids. However, our results also show that functional performance depends strongly on the type of reaction studied and, comparison with the average errors reported in the literature[21,22] shows that errors in the calculation of BHs and REs are higher for larger systems.

FIG. 2. Reaction energy (top left), overall barrier height (top right), forward reaction barrier height (bottom left), and reverse reaction barrier height (bottom right) mean absolute errors (MAEs) as a function of reaction type and density functional (using the Def2-QZVPP basis set). Open symbols represent the XDM-corrected version of each functional.
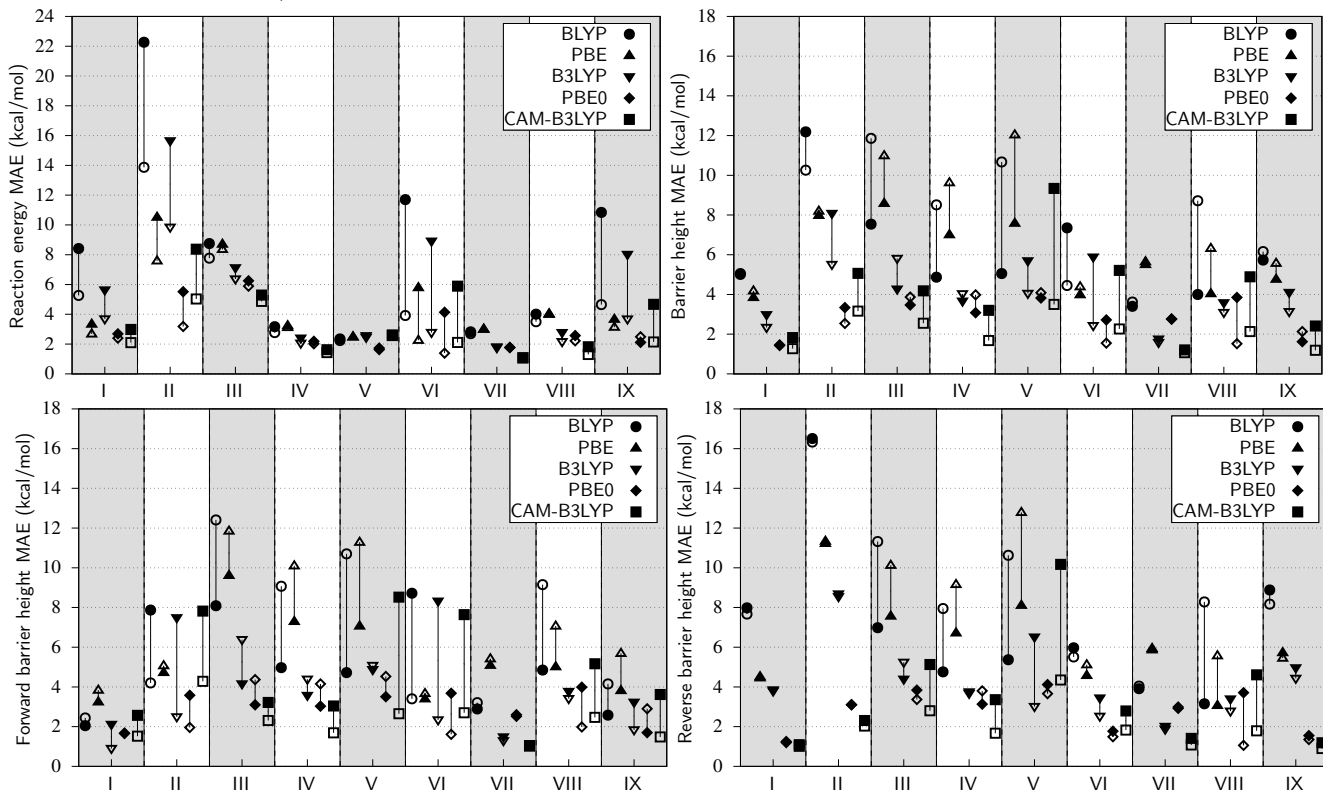
Assessment of basis set incompleteness potentials

One of our objectives in the construction of the BH9 set is to provide training data for the development of atom-centered potentials (ACPs).[55–57,157] ACPs are one-electron potentials that are designed to correct for the shortcomings of the DFT method to which they are applied. One particular flavor of ACPs are the basis set incompleteness potentials[55,56] (BSIPs) whose purpose is to minimize the basis set incompleteness error (BSIE) that originates from using small or minimal basis sets in DFT calculations. The application of BSIPs allows computing molecular properties with a quality similar to a complete basis set but at a much reduced computational cost.

The development of ACPs requires a relatively large training set of molecular properties. BSIPs, in particular, are constructed by minimizing the deviation between the BSIP-corrected small-basis-set values and the complete-basis-set values for a number of molecular properties. Since both the approximate and the reference molecular properties are calculated using the same functional and BSIE is mostly functional-independent, this ensures that BSIPs are mostly transferable between functionals, and are tied only to the basis set for which they were developed.[55]

The training set for the recently developed BSIPs contained only 316 REs and 102 BHs, out of a total of 9,372 molecular properties.[56] Therefore, it is interesting to examine whether BSIPs decrease BSIE in the calculation of REs and BHs by applying them to the BH9 set. For this test, we used the BSIPs from our previous work.[56] Of the 15 basis sets for which BSIPs were developed, only six had thermochemical data in their training set (6-31G*, 6-31+G*, 6-31+G**, Def2-SV(P), Def2-SVP, and pc-1), so we restrict our analysis to these basis sets. We chose PBE0-XDM as the base functional for this analysis in order to check the transferability of BSIPs across functionals. (These BSIPs were developed using B3LYP.[56])

The MAEs for the REs and BHs in the BH9 set using BSIP-corrected and uncorrected PBE0-XDM in combination with the aforementioned basis sets are shown in Table VI. The table shows two sets of MAEs with respect to different reference data: the DLPNO-CCSD(T)/CBS values ("Ref.") and our complete-basis-set PBE0-XDM estimate using the Def2-QZVPP basis set ("CBS"). Since the objective of BSIP development is to minimize BSIE, comparison with the CBS results is the purest measure of performance. The uncorrected MAEs ("Bare") in Table VI show that the magnitude of the BSIE on average is between

TABLE VI. Mean absolute errors (MAE) for the BH9 barrier heights and reaction energies of PBE0-XDM with several BSIP-corrected and uncorrected basis sets.[a]

		Reaction energies		Barrier heights	
		CBS[b]	Ref.[c]	CBS[b]	Ref.[c]
6-31G*	Bare	3.59	3.97	2.46	4.27
	BSIP	1.91	3.46	1.62	3.26
6-31+G*	Bare	2.49	3.01	1.48	3.30
	BSIP	0.89	2.65	0.75	2.83
6-31+G**	Bare	1.81	2.66	1.42	3.48
	BSIP	0.64	2.65	0.63	2.81
Def2-SV(P)	Bare	4.12	4.65	3.11	4.96
	BSIP	1.95	3.64	1.80	2.91
Def2-SVP	Bare	3.12	3.97	2.90	4.87
	BSIP	2.19	3.97	1.74	3.06
pc-1	Bare	2.42	2.86	2.60	4.80
	BSIP	1.41	3.17	1.32	3.18
Def2-QZVPP			2.74		2.85

[a] Units are kcal/mol. The statistics correspond to the whole BH9 set. [b] CBS = MAEs calculated with respect to our complete-basis-set estimate (Def2-QZVPP).
[c] Ref. = MAEs calculated with respect to the DLPNO-CCSD(T)/CBS reference data for the BH9.

1.4 kcal/mol and 4 kcal/mol, depending on the basis set, and that there are no significant differences between BHs and REs regarding BSIE. When BSIPs are applied, the MAEs with respect to the CBS values decreases in all cases, by up to 2 kcal/mol, bringing the results to a reasonably close agreement with the Def2-QZVPP results. The performance of BSIPs is better for the larger basis sets, 6-31+G* and 6-31+G**, where the MAEs with respect to the CBS reference are lower than 1 kcal/mol for both BHs and REs. There seems to be no salient differences between the effect of BSIPs on REs and BHs. These results are encouraging because of the aforementioned sparsity of thermochemical and kinetic data in the training set, which suggests that BSIPs have robust performance for systems significantly different from those in the training set. Also, because a functional different from PBE0-XDM was used in their development, our results suggest a strong transferability of BSIPs across functionals.

The MAEs between the small-basis-set BSIP-corrected and uncorrected PBE0-XDM results and the DLPNO-CCSD(T)/CBS data are also shown in Table VI ("Ref." column). In this case, the particular MAE values result from a combination of two errors: the uncorrected BSIE and the errors from the PBE0-XDM functional itself. Application of BSIPs reduces the MAEs in general to values that are close to the MAE of PBE0-XDM/Def2-QZVPP, particularly for the BHs, for which the BSIP-corrected MAEs are at most 0.41 kcal/mol above the Def2-QZVPP MAE. However, in some cases the MAE is unaffected or increases slightly due to favorable error cancellation in the uncorrected results.

CONCLUSIONS

In this article we introduce the BH9 set, an extensive and diverse benchmark dataset for reaction energies (REs) and barrier heights (BHs) in organic and bio-organic reactions. The BH9 set comprises 449 diverse reactions (449 REs and 898 BHs) involving relatively large molecular species (up to 71 atoms), similar to those found in thermochemical and mechanistic studies. The molecular species in BH9 comprise main-group elements, particularly those typically found in organic and bio-organic chemistry (H, C, N, O, F, P, S, and Cl) plus B and Si.

The computational level for the BH9 reference data is DLPNO-CCSD(T) combined with a focal-point approach in order to minimize errors from basis set incompleteness. We used a small subset of the BH9 composed of small molecular species to evaluate the errors introduced by our approximations and to estimate an error bar for the BH9 reference data. The DLPNO approximation is the main source of error, in comparison with basis set incompleteness. We estimate that the overall accuracy of the benchmark is in the vicinity of 1 kcal/mol or better.

The newly created BH9 was applied in two ways. First, we benchmarked a few popular density functionals used in the literature for calculating REs and BHs, as well as some XDM-corrected functionals to evaluate the effect of dispersion interactions on REs and BHs. In general, hybrid and range-separated hybrid functionals perform much better than GGA and meta-GGA functionals. The best performing functional is ωB97M-V with an MAE of 1.68 kcal/mol for reaction energies and 2.08 kcal/mol for barrier heights. The Minnesota functionals M05-2X, M06-2X as well as ωB97XD and PBE0-XDM show relatively good performance for both reaction energies and barrier heights, with MAEs between 2 and 3 kcal/mol for both properties. The XDM-corrected functional CAM-B3LYP-XDM, ωB97X-V and MN15 closely followed these functionals in terms of performance, with MAEs between 2 and 3.5 kcal/mol. We also verified that delocalization error is a major contribution to the BH and RE errors. However, for the reactions involving large molecular species (e.g. some pericyclic reactions), the incorrect treatment of dispersion seems to outweigh delocalization error for non-dispersion-corrected functionals.

Lastly, we applied the BH9 set to analyze the performance of our basis set incompleteness potentials (BSIPs) for REs and BHs in combination with a few double-ζ basis sets and the PBE0-XDM functional. We found that, despite the fact that thermochemical and kinetic data were only a small part of their training set and that they were developed using a different

functional (B3LYP), BSIPs performed excellently, reducing the discrepancy between the double-ζ and the complete-basis-set results by a factor of around 1.5 to 2. For BHs, the BSIP-corrected double-ζ MAEs were at most 0.41 kcal/mol higher than the Def2-QZVPP MAE, and the calculations were immensely less expensive. This confirms BSIPs are a robust way of minimizing basis set incompleteness from finite basis sets.

To our knowledge, BH9 is the most comprehensive BH and RE benchmark set to date. We hope that it will be useful to assess and develop new methods for thermochemical and kinetic work.

SUPPORTING INFORMATION

Table containing the list of reactions for the BH9 set organized by type, and the reference reaction energy and barrier heights. Plain-text db files for all reactions. Plain-text xyz files for all molecular structures involved in the reactions.

ACKNOWLEDGEMENTS

---

* ORCID:0000-0003-0982-3129
† Current address: Department of Chemistry, McGill University, 801 Sherbrooke St. West, Montréal, Québec, Canada H3A 0B8.
‡ aoterodelaroza@gmail.com
§ gino.dilabio@ubc.ca

[1] Laidler, K. *Chemical Kinetics*; Harper & Row, 1987.
[2] Truhlar, D. G.; Garrett, B. C.; Klippenstein, S. J. Current status of transition-state theory. *J. Phys. Chem.* **1996**, *100*, 12771–12800.
[3] Klippenstein, S. J.; Pande, V. S.; Truhlar, D. G. Chemical kinetics and mechanisms of complex systems: a perspective on recent theoretical advances. *J. Am. Chem. Soc.* **2014**, *136*, 528–546.
[4] Bachrach, S. M. Challenges in computational organic chemistry. *Wiley Interdiscip. Rev.: Comput. Mol. Sci.* **2014**, *4*, 482–487.
[5] Houk, K.; Liu, F. Holy grails for computational organic chemistry and biochemistry. *Acc. Chem. Res.* **2017**, *50*, 539–543.
[6] van der Kamp, M. W.; Mulholland, A. J. Combined quantum mechanics/molecular mechanics (QM/MM) methods in computational enzymology. *Biochemistry* **2013**, *52*, 2708–2728.
[7] Ahmadi, S.; Barrios Herrera, L.; Chehelamirani, M.; Hostaš, J.; Jalife, S.; Salahub, D. R. Multiscale modeling of enzymes: QM-cluster, QM/MM, and QM/MM/MD: A tutorial review. *Int. J. Quantum Chem.* **2018**, *118*, e25558.
[8] Himo, F. Recent trends in quantum chemical modeling of enzymatic reactions. *J. Am. Chem. Soc.* **2017**, *139*, 6780–6786.
[9] Quesne, M. G.; Borowski, T.; de Visser, S. P. Quantum mechanics/molecular mechanics modeling of enzymatic processes: Caveats and breakthroughs. *Chem. Eur. J.* **2016**, *22*, 2562–2581.
[10] Engkvist, O.; Norrby, P.-O.; Selmi, N.; Lam, Y.-h.; Peng, Z.; Sherer, E. C.; Amberg, W.; Erhard, T.; Smyth, L. A. Computational prediction of chemical reactions: current status and outlook. *Drug Discov. Today* **2018**, *23*, 1203–1218.
[11] Lam, Y.-h.; Abramov, Y.; Ananthula, R. S.; Elward, J. M.; Hilden, L. R.; Nilsson Lill, S. O.; Norrby, P.-O.; Ramirez, A.; Sherer, E. C.; Mustakis, J., et al. Applications of Quantum Chemistry in Pharmaceutical Process Development: Current State and Opportunities. *Org. Process Res. Dev.* **2020**, *24*, 1496–1507.
[12] Peterson, K. A.; Feller, D.; Dixon, D. A. Chemical accuracy in ab initio thermochemistry and spectroscopy: current strategies and future challenges. *Theor. Chem. Acc.* **2012**, *131*, 1–20.
[13] Karton, A.; Rabinovich, E.; Martin, J. M.; Ruscic, B. W4 theory for computational thermochemistry: In pursuit of confident sub-kJ/mol predictions. *J. Chem. Phys.* **2006**, *125*, 144108.
[14] Curtiss, L. A.; Redfern, P. C.; Raghavachari, K. Gaussian-4 theory. *J. Chem. Phys.* **2007**, *126*, 084108.
[15] Harding, M. E.; Vázquez, J.; Ruscic, B.; Wilson, A. K.; Gauss, J.; Stanton, J. F. High-accuracy extrapolated ab initio thermochemistry. III. Additional improvements and overview. *J. Chem. Phys.* **2008**, *128*, 114111.
[16] Karton, A. A computational chemist's guide to accurate thermochemistry for organic molecules. *Wiley Interdiscip. Rev.: Comput. Mol. Sci.* **2016**, *6*, 292–310.
[17] Karton, A.; Sylvetsky, N.; Martin, J. M. W4-17: A diverse and high-confidence dataset of atomization energies for benchmarking high-level electronic structure methods. *J. Comput. Chem.* **2017**, *38*, 2063–2075.
[18] Chan, B. How to computationally calculate thermochemical properties objectively, accurately, and as economically as possible. *Pure Appl. Chem.* **2017**, *89*, 699–713.
[19] Bistoni, G.; Polyak, I.; Sparta, M.; Thiel, W.; Neese, F. Toward accurate QM/MM reaction barriers with large QM regions using domain based pair natural orbital coupled cluster theory. *J. Chem. Theory Comput.* **2018**,

14, 3524–3531.

[20] Deglmann, P.; Schäfer, A.; Lennartz, C. Application of quantum calculations in the chemical industry—An overview. *Int. J. Quantum Chem.* **2015**, *115*, 107–136.

[21] Mardirossian, N.; Head-Gordon, M. Thirty years of density functional theory in computational chemistry: an overview and extensive assessment of 200 density functionals. *Mol. Phys.* **2017**, *115*, 2315–2372.

[22] Goerigk, L.; Hansen, A.; Bauer, C.; Ehrlich, S.; Najibi, A.; Grimme, S. A look at the density functional theory zoo with the advanced GMTKN55 database for general main group thermochemistry, kinetics and noncovalent interactions. *Phys. Chem. Chem. Phys.* **2017**, *19*, 32184–32215.

[23] Goerigk, L.; Mehta, N. A trip to the density functional theory zoo: warnings and recommendations for the user. *Aust. J. Chem.* **2019**, *72*, 563–573.

[24] Morgante, P.; Peverati, R. ACCDB: A collection of chemistry databases for broad computational purposes. *J. Comput. Chem.* **2019**, *40*, 839–848.

[25] Yu, H. S.; Zhang, W.; Verma, P.; He, X.; Truhlar, D. G. Nonseparable exchange–correlation functional for molecules, including homogeneous catalysis involving transition metals. *Phys. Chem. Chem. Phys.* **2015**, *17*.

[26] Yu, H. S.; He, X.; Truhlar, D. G. MN15-L: A new local exchange-correlation functional for Kohn–Sham density functional theory with broad accuracy for atoms, molecules, and solids. *J. Chem. Theory Comput.* **2016**, *12*, 1280–1293.

[27] Haoyu, S. Y.; He, X.; Li, S. L.; Truhlar, D. G. MN15: A Kohn–Sham global-hybrid exchange–correlation density functional with broad accuracy for multi-reference and single-reference systems and noncovalent interactions. *Chem. Sci.* **2016**, *7*, 5032–5051.

[28] Johnson, E. R.; Mori-Sánchez, P.; Cohen, A. J.; Yang, W. Delocalization errors in density functionals and implications for main-group thermochemistry. *J. Chem. Phys.* **2008**, *129*, 204112.

[29] Yu, L.-J.; Sarrami, F.; O'Reilly, R. J.; Karton, A. Reaction barrier heights for cycloreversion of heterocyclic rings: An Achilles' heel for DFT and standard ab initio procedures. *Chem. Phys.* **2015**, *458*, 1–8.

[30] Lonsdale, R.; Harvey, J. N.; Mulholland, A. J. Inclusion of dispersion effects significantly improves accuracy of calculated reaction barriers for cytochrome P450 catalyzed reactions. *J. Phys. Chem. Lett.* **2010**, *1*, 3232–3237.

[31] Sandler, I.; Chen, J.; Taylor, M.; Sharma, S.; Ho, J. Accuracy of DLPNO-CCSD (T): Effect of Basis Set and System Size. *J. Phys. Chem. A* **2021**, *125*, 1553–1563.

[32] Wappett, D. A.; Goerigk, L. Toward a quantum-chemical benchmark set for enzymatically catalyzed reactions: important steps and insights. *J. Phys. Chem. A* **2019**, *123*, 7057–7074.

[33] Wappett, D. A.; Goerigk, L. A guide to benchmarking enzymatically catalysed reactions: the importance of accurate reference energies and the chemical environment. *Theor. Chem. Acc.* **2021**, *140*, 1–15.

[34] Zheng, J.; Zhao, Y.; Truhlar, D. G. Representative benchmark suites for barrier heights of diverse reaction types and assessment of electronic structure methods for thermochemical kinetics. *J. Chem. Theory Comput.*

2007, *3*, 569–582.

[35] Karton, A.; Tarnopolsky, A.; Lamére, J.-F.; Schatz, G. C.; Martin, J. M. Highly accurate first-principles benchmark data sets for the parametrization and validation of density functional and other approximate methods. Derivation of a robust, generally applicable, double-hybrid functional for thermochemistry and thermochemical kinetics. *J. Phys. Chem. A* **2008**, *112*, 12868–12886.

[36] Zhao, Y.; González-García, N.; Truhlar, D. G. Benchmark database of barrier heights for heavy atom transfer, nucleophilic substitution, association, and unimolecular reactions and its use to test theoretical methods. *J. Phys. Chem. A* **2005**, *109*, 2012–2018.

[37] Zhao, Y.; Lynch, B. J.; Truhlar, D. G. Multi-coefficient extrapolated density functional theory for thermochemistry and thermochemical kinetics. *Phys. Chem. Chem. Phys.* **2005**, *7*, 43–52.

[38] Chan, B.; Simmie, J. M. Barriometry–an enhanced database of accurate barrier heights for gas-phase reactions. *Phys. Chem. Chem. Phys.* **2018**, *20*, 10732–10740.

[39] Goerigk, L.; Sharma, R. The INV24 test set: how well do quantum-chemical methods describe inversion and racemization barriers? *Can. J. Chem.* **2016**, *94*, 1133–1143.

[40] Karton, A.; Goerigk, L. Accurate reaction barrier heights of pericyclic reactions: Surprisingly large deviations for the CBS-QB3 composite method and their consequences in DFT benchmark studies. *J. Comput. Chem.* **2015**, *36*, 622–632.

[41] Karton, A.; O'Reilly, R. J.; Radom, L. Assessment of theoretical procedures for calculating barrier heights for a diverse set of water-catalyzed proton-transfer reactions. *J. Phys. Chem. A* **2012**, *116*, 4211–4221.

[42] Karton, A.; O'Reilly, R. J.; Chan, B.; Radom, L. Determination of Barrier Heights for Proton Exchange in Small Water, Ammonia, and Hydrogen Fluoride Clusters with G4 (MP2)-Type, MP n, and SCS-MPn Procedures-A Caveat. *J. Chem. Theory Comput.* **2012**, *8*, 3128–3136.

[43] Grambow, C. A.; Pattanaik, L.; Green, W. H. Reactants, products, and transition states of elementary chemical reactions based on quantum chemistry. *Sci. Data* **2020**, *7*, 1–8.

[44] von Rudorff, G. F.; Heinen, S. N.; Bragato, M.; von Lilienfeld, O. A. Thousands of reactants and transition states for competing E2 and S2 reactions. *Mach. Learn. Sci. Technol.* **2020**, *1*, 045026.

[45] Kromann, J. C.; Christensen, A. S.; Cui, Q.; Jensen, J. H. Towards a barrier height benchmark set for biologically relevant systems. *PeerJ* **2016**, *4*, e1994.

[46] Riplinger, C.; Neese, F. An efficient and near linear scaling pair natural orbital based local coupled cluster method. *J. Chem. Phys.* **2013**, *138*, 034106.

[47] Riplinger, C.; Sandhoefer, B.; Hansen, A.; Neese, F. Natural triple excitations in local coupled cluster calculations with pair natural orbitals. *J. Chem. Phys.* **2013**, *139*, 134101.

[48] Liakos, D. G.; Sparta, M.; Kesharwani, M. K.; Martin, J. M.; Neese, F. Exploring the accuracy limits of local pair natural orbital coupled-cluster theory. *J. Chem. Theory Comput.* **2015**, *11*, 1525–1539.

[49] Riplinger, C.; Pinski, P.; Becker, U.; Valeev, E. F.; Neese, F. Sparse maps-A systematic infrastructure for reduced-scaling electronic structure methods. II. Linear scaling domain based pair natural orbital coupled cluster theory. *J. Chem. Phys.* **2016**, *144*, 024109.

[50] Saitow, M.; Becker, U.; Riplinger, C.; Valeev, E. F.; Neese, F. A new near-linear scaling, efficient and accurate, open-shell domain-based local pair natural orbital coupled cluster singles and doubles theory. *J. Chem. Phys.* **2017**, *146*, 164105.

[51] Guo, Y.; Riplinger, C.; Becker, U.; Liakos, D. G.; Minenkov, Y.; Cavallo, L.; Neese, F. Communication: An improved linear scaling perturbative triples correction for the domain based local pair-natural orbital based singles and doubles coupled cluster method [DLPNO-CCSD (T)]. *J. Chem. Phys.* **2018**, *148*, 011101.

[52] Paiva, P.; Ramos, M. J.; Fernandes, P. A. Assessing the validity of DLPNO-CCSD(T) in the calculation of activation and reaction energies of ubiquitous enzymatic reactions. *J. Comput. Chem.* **2020**, *41*, 2459–2468.

[53] Iron, M. A.; Janes, T. Evaluating transition metal barrier heights with the latest density functional theory exchange–correlation functionals: the MOBH35 benchmark database. *J. Phys. Chem. A* **2019**, *123*, 3761–3781.

[54] Dohm, S.; Hansen, A.; Steinmetz, M.; Grimme, S.; Checinski, M. P. Comprehensive thermochemical benchmark set of realistic closed-shell metal organic reactions. *J. Chem. Theory Comput.* **2018**, *14*, 2596–2608.

[55] Otero-de-la-Roza, A.; DiLabio, G. A. Transferable atom-centered potentials for the correction of basis set incompleteness errors in density-functional theory. *J. Chem. Theory Comput.* **2017**, *13*, 3505–3524.

[56] Otero-de-la-Roza, A.; DiLabio, G. A. Improved basis-set incompleteness potentials for accurate dft calculations in large systems. *J. Chem. Theory Comput.* **2020**, *16*, 4176–4191.

[57] Prasad, V. K.; Otero-de-la-Roza, A.; DiLabio, G. A. Atom-centered potentials with dispersion-corrected minimal basis set Hartree-Fock: an efficient and accurate computational approach for large molecular systems. *J. Chem. Theory Comput.* **2018**, *14*, 726–738.

[58] Prasad, V. K.; Otero-de La-Roza, A.; DiLabio, G. A. PEPCONF, a diverse data set of peptide conformational energies. *Sci. Data* **2019**, *6*, 1–9.

[59] Prasad, V. K.; Khalilian, M. H.; Otero-de-la-Roza, A.; DiLabio, G. A. BSE49, a diverse, high-quality benchmark dataset of separation energies of chemical bonds. *Sci. Data* **2021**, (submitted).

[60] Chan, B. Formulation of Small Test Sets Using Large Test Sets for Efficient Assessment of Quantum Chemistry Methods. *J. Chem. Theory Comput.* **2018**, *14*, 4254–4262.

[61] Ribeiro, A. J. M.; Holliday, G. L.; Furnham, N.; Tyzack, J. D.; Ferris, K.; Thornton, J. M. Mechanism and Catalytic Site Atlas (M-CSA): a database of enzyme reaction mechanisms and active sites. *Nucleic Acids Res.* **2018**, *46*, D618–D623.

[62] Newcomb, M. In *Encyclopedia of Radicals in Chemistry, Biology and Materials*; Chatgilialoglu, C., Studer, A., Eds.; Wiley Online Library, 2012.

[63] Mackie, I. D.; DiLabio, G. A. Ring-opening radical clock reactions: many density functionals have difficulty keeping time. *Org. Biomol. Chem.* **2011**, *9*, 3158–3164.

[64] Lucas, M. d. F.; Ramos, M. J. Theoretical study of the suicide inhibition mechanism of the enzyme pyruvate formate lyase by methacrylate. *J. Am. Chem. Soc.* **2005**, *127*, 6902–6909.

[65] Zou, Y.; Xue, X.-S.; Deng, Y.; Smith III, A. B.; Houk, K. Factors Controlling Reactivity in the Hydrogen Atom Transfer and Radical Addition Steps of a Radical Relay Cascade. *Org. Lett.* **2019**, *21*, 5894–5897.

[66] Romero-Silva, A.; Mora-Diez, N.; Alvarez-Idaboy, J. R. Theoretical study of the reactivity and selectivity of various free radicals with cysteine residues. *ACS Omega* **2018**, *3*, 16519–16528.

[67] Hayden, A. E.; Paton, R. S.; Becker, J.; Lim, Y. H.; Nicolaou, K.; Houk, K. Origins of regioselectivity of Diels- Alder reactions for the synthesis of bisanthraquinone antibiotic BE-43472B. *J. Org. Chem.* **2010**, *75*, 922–928.

[68] Lan, Y.; Danheiser, R. L.; Houk, K. Why Nature Eschews the Concerted [2+ 2+ 2] Cycloaddition of a Nonconjugated Cyanodiyne. Computational Study of a Pyridine Synthesis Involving an Ene–Diels–Alder–Bimolecular Hydrogen-Transfer Mechanism. *J. Org. Chem.* **2012**, *77*, 1533–1538.

[69] Zheng, Y.; Thiel, W. Computational insights into an enzyme-catalyzed [4+ 2] cycloaddition. *J. Org. Chem.* **2017**, *82*, 13563–13571.

[70] Sato, M.; Yagishita, F.; Mino, T.; Uchiyama, N.; Patel, A.; Chooi, Y.-H.; Goda, Y.; Xu, W.; Noguchi, H.; Yamamoto, T., et al. Involvement of lipocalin-like CghA in decalin-forming stereoselective intramolecular [4+ 2] cycloaddition. *ChemBioChem* **2015**, *16*, 2294.

[71] Zhang, B.; Wang, K. B.; Wang, W.; Wang, X.; Liu, F.; Zhu, J.; Shi, J.; Li, L. Y.; Han, H.; Xu, K., et al. Enzyme-catalysed [6+ 4] cycloadditions in the biosynthesis of natural products. *Nature* **2019**, *568*, 122–126.

[72] Maiga-Wandiam, B.; Corbu, A.; Massiot, G.; Sautel, F.; Yu, P.; Lin, B. W.-Y.; Houk, K. N.; Cossy, J. Intramolecular Diels–Alder Approaches to the Decalin Core of Verongidolide: The Origin of the exo-Selectivity, a DFT Analysis. *J. Org. Chem.* **2018**, *83*, 5975–5985.

[73] Byrne, M. J.; Lees, N. R.; Han, L.-C.; van der Kamp, M. W.; Mulholland, A. J.; Stach, J. E.; Willis, C. L.; Race, P. R. The catalytic mechanism of a natural Diels–Alderase revealed in molecular detail. *J. Am. Chem. Soc.* **2016**, *138*, 6095–6098.

[74] He, C. Q.; Chen, T. Q.; Patel, A.; Karabiyikoglu, S.; Merlic, C. A.; Houk, K. Distortion, tether, and entropy effects on transannular Diels–Alder cycloaddition reactions of 10–18-membered rings. *J. Org. Chem.* **2015**, *80*, 11039–11047.

[75] Yu, P.; Patel, A.; Houk, K. Transannular [6+ 4] and ambimodal cycloaddition in the biosynthesis of heronamide A. *J. Am. Chem. Soc.* **2015**, *137*, 13518–13523.

[76] Pham, H. V.; Paton, R. S.; Ross, A. G.; Danishefsky, S. J.; Houk, K. Intramolecular Diels–Alder reactions of cycloalkenones: stereoselectivity, Lewis acid acceleration, and halogen substituent effects. *J. Am. Chem. Soc.* **2014**, *136*, 2397–2403.

[77] Duan, A.; Yu, P.; Liu, F.; Qiu, H.; Gu, F. L.; Doyle, M. P.; Houk, K. Diazo esters as dienophiles in intramolecular (4+ 2) cycloadditions: Computational explorations of mechanism. *J. Am. Chem. Soc.* **2017**, *139*, 2766–2770.

[78] Fell, J. S.; Lopez, S. A.; Higginson, C. J.; Finn, M.; Houk, K. Theoretical Analysis of the Retro-Diels–Alder Reactivity of Oxanorbornadiene Thiol and Amine Adducts. *Org. Lett.* **2017**, *19*, 4504–4507.

[79] Levandowski, B. J.; Herath, D.; Gallup, N. M.; Houk, K. Origin of π-Facial Stereoselectivity in Thiophene 1-Oxide Cycloadditions. *J. Org. Chem.* **2018**, *83*, 2611–2616.

[80] Scholl, K.; Dillashaw, J.; Timpy, E.; Lam, Y.-h.; DeRatt, L.; Benton, T. R.; Powell, J. P.; Houk, K.; Morgan, J. B. Quinine-Promoted, Enantioselective Boron-Tethered Diels–Alder Reaction by Anomeric Control of Transition-State Conformation. *J. Org. Chem.* **2018**, *83*, 5756–5765.

[81] Suh, S.-E.; Chen, S.; Houk, K.; Chenoweth, D. M. The mechanism of the triple aryne–tetrazine reaction cascade: theory and experiment. *Chem. Sci.* **2018**, *9*, 7688–7693.

[82] Tan, D.; Jamieson, C. S.; Ohashi, M.; Tang, M.-C.; Houk, K.; Tang, Y. Genome-mined Diels–Alderase catalyzes formation of the cis-octahydrodecalins of varicidin A and B. *J. Am. Chem. Soc.* **2019**, *141*, 769–773.

[83] Schmidt, Y.; Lam, J. K.; Pham, H. V.; Houk, K.; Vanderwal, C. D. Studies on the Himbert intramolecular Arene/Allene Diels–alder cycloaddition. Mechanistic studies and expansion of scope to all-carbon tethers. *J. Am. Chem. Soc.* **2013**, *135*, 7339–7348.

[84] Liang, Y.; Mackey, J. L.; Lopez, S. A.; Liu, F.; Houk, K. Control and design of mutual orthogonality in bioorthogonal cycloadditions. *J. Am. Chem. Soc.* **2012**, *134*, 17904–17907.

[85] Liu, S.; Lei, Y.; Qi, X.; Lan, Y. Reactivity for the Diels–Alder reaction of cumulenes: a distortion-interaction analysis along the reaction pathway. *J. Phys. Chem. A* **2014**, *118*, 2638–2645.

[86] Ma, Z.-X.; Patel, A.; Houk, K.; Hsung, R. P. Highly Torquoselective Electrocyclizations and Competing 1, 7-Hydrogen Shifts of 1-Azatrienes with Silyl Substitution at the Allylic Carbon. *Org. Lett.* **2015**, *17*, 2138–2141.

[87] Ohashi, M.; Liu, F.; Hai, Y.; Chen, M.; Tang, M.-c.; Yang, Z.; Sato, M.; Watanabe, K.; Houk, K.; Tang, Y. SAM-dependent enzyme-catalysed pericyclic reactions in natural product biosynthesis. *Nature* **2017**, *549*, 502–506.

[88] Yang, Z.; Dong, X.; Yu, Y.; Yu, P.; Li, Y.; Jamieson, C.; Houk, K. Relationships between product ratios in ambimodal pericyclic reactions and bond lengths in transition structures. *J. Am. Chem. Soc.* **2018**, *140*, 3061–3067.

[89] Xue, X.-S.; Jamieson, C. S.; Garcia-Borràs, M.; Dong, X.; Yang, Z.; Houk, K. Ambimodal trispericyclic transition state and dynamic control of periselectivity. *J. Am. Chem. Soc.* **2019**, *141*, 1217–1221.

[90] Wiest, O.; Houk, K. Stabilization of the transition state of the chorismate-prephenate rearrangement: An ab initio study of enzyme and antibody catalysis. *J. Am. Chem. Soc.* **1995**, *117*, 11628–11639.

[91] Scott, S. K.; Sanders, J. N.; White, K. E.; Yu, R. A.; Houk, K.; Grenning, A. J. Controlling, understanding, and redirecting the thermal rearrangement of 3, 3-dicyano-1, 5-enynes. *J. Am. Chem. Soc.* **2018**, *140*, 16134–16139.

[92] Boon, B. A.; Green, A. G.; Liu, P.; Houk, K.; Merlic, C. A. Using ring strain to control 4π-electrocyclization reactions: torquoselectivity in ring closing of medium-ring dienes and ring opening of bicyclic cyclobutenes. *J. Org. Chem.* **2017**, *82*, 4613–4624.

[93] Patel, A.; Barcan, G. A.; Kwon, O.; Houk, K. Origins of 1, 6-Stereoinduction in Torquoselective 6π Electrocyclizations. *J. Am. Chem. Soc.* **2013**, *135*, 4878–4883.

[94] Sader, C. A.; Houk, K. A Theoretical Study of Cyclohexyne Addition to Carbonyl–Cα Bonds: Allowed and Forbidden Electrocyclic and Nonpericyclic Ring-Openings of Strained Cyclobutenes. *J. Org. Chem.* **2012**, *77*, 4939–4948.

[95] Hong, X.; Liang, Y.; Griffith, A. K.; Lambert, T. H.; Houk, K. Distortion-accelerated cycloadditions and strain-release-promoted cycloreversions in the organocatalytic carbonyl-olefin metathesis. *Chem. Sci.* **2014**, *5*, 471–475.

[96] Xie, S.; Lopez, S. A.; Ramström, O.; Yan, M.; Houk, K. 1, 3-Dipolar cycloaddition reactivities of perfluorinated aryl azides with enamines and strained dipolarophiles. *J. Am. Chem. Soc.* **2015**, *137*, 2958–2966.

[97] Krenske, E. H.; Patel, A.; Houk, K. Does nature click? Theoretical prediction of an enzyme-catalyzed transannular 1, 3-dipolar cycloaddition in the biosynthesis of lycojaponicumins A and B. *J. Am. Chem. Soc.* **2013**, *135*, 17638–17642.

[98] Çelebi-Ölçüm, N.; Lam, Y.-h.; Richmond, E.; Ling, K. B.; Smith, A. D.; Houk, K. N. Pericyclic Cascade with Chirality Transfer: Reaction Pathway and Origin of Enantioselectivity of the Hetero-Claisen Approach to Oxindoles. *Angew. Chem. Intl. Ed.* **2011**, *50*, 11478–11482.

[99] Hamlin, T. A.; Kelly, C. B.; Ovian, J. M.; Wiles, R. J.; Tilley, L. J.; Leadbeater, N. E. Toward a unified mechanism for oxoammonium salt-mediated oxidation reactions: a theoretical and experimental study using a hydride transfer model. *J. Org. Chem.* **2015**, *80*, 8150–8167.

[100] Vitkovskaya, N. M.; Kobychev, V. B.; Bobkov, A. S.; Orel, V. B.; Schmidt, E. Y.; Trofimov, B. A. Nucleophilic Addition of Ketones To Acetylenes and Allenes: A Quantum-Chemical Insight. *J. Org. Chem.* **2017**, *82*, 12467–12476.

[101] Kister, J.; Ess, D. H.; Roush, W. R. Enantio-and Diastereoselective Synthesis of syn-β-Hydroxy-α-vinyl Carboxylic Esters via Reductive Aldol Reactions of Ethyl Allenecarboxylate with 10-TMS-9-Borabicyclo [3.3. 2] decane and DFT Analysis of the Hydroboration Pathway. *Org. Lett.* **2013**, *15*, 5436–5439.

[102] Johnson, E. R.; Clarkin, O. J.; Dale, S. G.; DiLabio, G. A. Kinetics of the addition of olefins to Si-centered radicals: the critical role of dispersion interactions revealed by theory and experiment. *J. Phys. Chem. A* **2015**, *119*, 5883–5888.

[103] Zhang, Z.; Collum, D. B. Wittig Rearrangements of Boron-Based Oxazolidinone Enolates. *J. Org. Chem.*

2019, *84*, 10892–10900.

[104] Liu, W.-B.; Schuman, D. P.; Yang, Y.-F.; Toutov, A. A.; Liang, Y.; Klare, H. F.; Nesnas, N.; Oestreich, M.; Blackmond, D. G.; Virgil, S. C., et al. Potassium tert-butoxide-catalyzed dehydrogenative C–H silylation of heteroaromatics: a combined experimental and computational mechanistic study. *J. Am. Chem. Soc.* **2017**, *139*, 6867–6879.

[105] D'Alfonso, C.; Bietti, M.; DiLabio, G. A.; Lanzalunga, O.; Salamone, M. Reactions of the Phthalimide N-Oxyl Radical (PINO) with Activated Phenols: The Contribution of π-Stacking Interactions to Hydrogen Atom Transfer Rates. *J. Org. Chem.* **2013**, *78*, 1026–1037.

[106] DiLabio, G. A.; Franchi, P.; Lanzalunga, O.; Lapi, A.; Lucarini, F.; Lucarini, M.; Mazzonna, M.; Prasad, V. K.; Ticconi, B. Hydrogen atom transfer (HAT) processes promoted by the quinolinimide-N-oxyl radical. A kinetic and theoretical study. *J. Org. Chem.* **2017**, *82*, 6133–6141.

[107] Chan, B.; Gill, P. M.; Kimura, M. Assessment of DFT methods for transition metals with the TMC151 compilation of data sets and comparison with accuracies for main-group chemistry. *J. Chem. Theory Comput.* **2019**, *15*, 3610–3622.

[108] Chan, B. Assessment and development of DFT with the expanded CUAGAU-2 set of group-11 cluster systems. *Int. J. Quantum Chem.* **2021**, *121*, e26453.

[109] Becke, A. D. Density-functional exchange-energy approximation with correct asymptotic behavior. *Phys. Rev. A* **1988**, *38*, 3098.

[110] Lee, C.; Yang, W.; Parr, R. G. Development of the Colle-Salvetti correlation-energy formula into a functional of the electron density. *Phys. Rev. B* **1988**, *37*, 785.

[111] Perdew, J.; Burke, K.; Ernzerhof, M. Generalized gradient approximation made simple. *Phys. Rev. Lett.* **1996**, *77*, 3865–3868.

[112] Tao, J.; Perdew, J. P.; Staroverov, V. N.; Scuseria, G. E. Climbing the density functional ladder: Nonempirical meta–generalized gradient approximation designed for molecules and solids. *Phys. Rev. Lett.* **2003**, *91*, 146401.

[113] Perdew, J. P.; Ruzsinszky, A.; Csonka, G. I.; Constantin, L. A.; Sun, J. Workhorse semilocal density functional for condensed matter physics and quantum chemistry. *Phys. Rev. Lett.* **2009**, *103*, 026403.

[114] Yu, H. S.; He, X.; Truhlar, D. G. MN15-L: A new local exchange-correlation functional for Kohn–Sham density functional theory with broad accuracy for atoms, molecules, and solids. *J. Chem. Theory Comput.* **2016**, *12*, 1280–1293.

[115] Mardirossian, N.; Head-Gordon, M. Mapping the genome of meta-generalized gradient approximation density functionals: The search for B97M-V. *J. Chem. Phys.* **2015**, *142*, 074111.

[116] Becke, A. D. Density-functional thermochemistry. III. The role of exact exchange. *J. Chem. Phys.* **1993**, *98*, 5648–5652.

[117] Adamo, C.; Barone, V. Toward reliable density functional methods without adjustable parameters: The PBE0 model. *J. Chem. Phys.* **1999**, *110*, 6158–6170.

[118] Becke, A. D. A new mixing of Hartree–Fock and local density-functional theories. *J. Chem. Phys.* **1993**, *98*, 1372.

[119] Zhao, Y.; Schultz, N. E.; Truhlar, D. G. Design of density functionals by combining the method of constraint satisfaction with parametrization for thermochemistry, thermochemical kinetics, and noncovalent interactions. *J. Chem. Theory Comput.* **2006**, *2*, 364–382.

[120] Zhao, Y.; Truhlar, D. G. The M06 suite of density functionals for main group thermochemistry, thermochemical kinetics, noncovalent interactions, excited states, and transition elements: two new functionals and systematic testing of four M06-class functionals and 12 other functionals. *Theor. Chem. Acc.* **2008**, *120*, 215–241.

[121] Haoyu, S. Y.; He, X.; Li, S. L.; Truhlar, D. G. MN15: A Kohn–Sham global-hybrid exchange–correlation density functional with broad accuracy for multi-reference and single-reference systems and noncovalent interactions. *Chem. Sci.* **2016**, *7*, 5032–5051.

[122] Yanai, T.; Tew, D. P.; Handy, N. C. A new hybrid exchange-correlation functional using the Coulomb-attenuating method (CAM-B3LYP). *Chem. Phys. Lett.* **2004**, *393*, 51–57.

[123] Vydrov, O. A.; Scuseria, G. E. Assessment of a long-range corrected hybrid functional. *J. Chem. Phys.* **2006**, *125*, 234109.

[124] Vydrov, O. A.; Heyd, J.; Krukau, A. V.; Scuseria, G. E. Importance of short-range versus long-range Hartree-Fock exchange for the performance of hybrid density functionals. *J. Chem. Phys.* **2006**, *125*, 074106.

[125] Chai, J.-D.; Head-Gordon, M. Systematic optimization of long-range corrected hybrid density functionals. *J. Chem. Phys.* **2008**, *128*, 084106.

[126] Chai, J.-D.; Head-Gordon, M. Long-range corrected hybrid density functionals with damped atom–atom dispersion corrections. *Phys. Chem. Chem. Phys.* **2008**, *10*, 6615–6620.

[127] Mardirossian, N.; Head-Gordon, M. ω B97M-V: A combinatorially optimized, range-separated hybrid, meta-GGA density functional with VV10 nonlocal correlation. *J. Chem. Phys.* **2016**, *144*, 214110.

[128] Mardirossian, N.; Head-Gordon, M. ωB97X-V: A 10-parameter, range-separated hybrid, generalized gradient approximation density functional with nonlocal correlation, designed by a survival-of-the-fittest strategy. *Phys. Chem. Chem. Phys.* **2014**, *16*, 9904–9924.

[129] Becke, A. D.; Johnson, E. R. Exchange-Hole Dipole Moment and the Dispersion Interaction Revisited. *J. Chem. Phys.* **2007**, *127*, 154108.

[130] Otero-de-la-Roza, A.; Johnson, E. R. Non-Covalent Interactions and Thermochemistry using XDM-Corrected Hybrid and Range-Separated Hybrid Density Functionals. *J. Chem. Phys.* **2013**, *138*, 204109.

[131] The postg program is freely available from `https://github.com/aoterodelaroza/postg`.

[132] The canoical XDM coefficients can be found at `http://schooner.chem.dal.ca` and also in the xdm.param file of the postg distribution.

[133] Grimme, S.; Antony, J.; Ehrlich, S.; Krieg, H. A consistent and accurate ab initio parametrization of density functional dispersion correction (DFT-D) for the 94 elements H-Pu. *J. Chem. Phys.* **2010**, *132*, 154104.

[134] Francl, M. M.; Pietro, W. J.; Hehre, W. J.; Binkley, J. S.; Gordon, M. S.; DeFrees, D. J.; Pople, J. A. Self-consistent molecular orbital methods. XXIII. A polarization-type basis set for second-row elements. *J. Chem. Phys.* **1982**, *77*, 3654–3665.

[135] Hariharan, P. C.; Pople, J. A. The influence of polarization functions on molecular orbital hydrogenation energies. *Theor. Chim. Acta* **1973**, *28*, 213–222.

[136] Hehre, W. J.; Ditchfield, R.; Pople, J. A. Self-consistent molecular orbital methods. XII. Further extensions of Gaussian—type basis sets for use in molecular orbital studies of organic molecules. *J. Chem. Phys.* **1972**, *56*, 2257–2261.

[137] Weigend, F.; Ahlrichs, R. Balanced basis sets of split valence, triple zeta valence and quadruple zeta valence quality for H to Rn: Design and assessment of accuracy. *Phys. Chem. Chem. Phys.* **2005**, *7*, 3297–3305.

[138] Jensen, F. Polarization consistent basis sets: Principles. *J. Chem. Phys.* **2001**, *115*, 9113–9125.

[139] Jensen, F. Polarization consistent basis sets. II. Estimating the Kohn–Sham basis set limit. *J. Chem. Phys.* **2002**, *116*, 7372–7379.

[140] Jensen, F. Polarization consistent basis sets. III. The importance of diffuse functions. *J. Chem. Phys.* **2002**, *117*, 9234–9240.

[141] Jensen, F.; Helgaker, T. Polarization consistent basis sets. V. The elements Si–Cl. *J. Chem. Phys.* **2004**, *121*, 3463–3470.

[142] Karton, A. Highly accurate CCSDT(Q)/CBS reaction barrier heights for a diverse set of transition structures: basis set convergence and cost-effective approaches for estimating post-CCSD(T) contributions. *J. Phys. Chem. A* **2019**, *123*, 6720–6732.

[143] East, A. L.; Allen, W. D. The heat of formation of NCO. *J. Chem. Phys.* **1993**, *99*, 4638–4650.

[144] East, A. L.; Johnson, C. S.; Allen, W. D. Characterization of the $\tilde{X}^1 A'$ state of isocyanic acid. *J. Chem. Phys.* **1993**, *98*, 1299–1328.

[145] Helgaker, T.; Klopper, W.; Koch, H.; Noga, J. Basis-set convergence of correlated calculations on water. *J. Chem. Phys.* **1997**, *106*, 9639–9646.

[146] Halkier, A.; Helgaker, T.; Jørgensen, P.; Klopper, W.; Koch, H.; Olsen, J.; Wilson, A. K. Basis-set convergence in correlated calculations on Ne, N2, and H2O. *Chem. Phys. Lett.* **1998**, *286*, 243–252.

[147] Karton, A.; Martin, J. M. Comment on: Estimating the Hartree–Fock limit from finite basis set calculations [Jensen F (2005) Theor Chem Acc 113: 267]. *Theor. Chem. Acc.* **2006**, *115*, 330–333.

[148] Jensen, F. Estimating the Hartree—Fock limit from finite basis set calculations. *Theor. Chem. Acc.* **2005**, *113*, 267–273.

[149] Burns, L. A.; Marshall, M. S.; Sherrill, C. D. Appointing silver and bronze standards for noncovalent interactions: A comparison of spin-component-scaled (SCS), explicitly correlated (F12), and specialized wavefunction approaches. *J. Chem. Phys.* **2014**, *141*, 234111.

[150] Papajak, E.; Truhlar, D. G. What are the most efficient basis set strategies for correlated wave function calculations of reaction energies and barrier heights? *J. Chem. Phys.* **2012**, *137*, 064110.

[151] Goerigk, L.; Grimme, S. A thorough benchmark of density functional methods for general main group thermochemistry, kinetics, and noncovalent interactions. *Phys. Chem. Chem. Phys.* **2011**, *13*, 6670–6688.

[152] Mardirossian, N.; Head-Gordon, M. How accurate are the Minnesota density functionals for noncovalent interactions, isomerization energies, thermochemistry, and barrier heights involving molecules composed of main-group elements? *J. Chem. Theory Comput.* **2016**, *12*, 4303–4325.

[153] Goerigk, L.; Kruse, H.; Grimme, S. Benchmarking density functional methods against the S66 and S66x8 datasets for non-covalent interactions. *Chem. Phys. Chem* **2011**, *12*, 3421–3433.

[154] Grimme, S.; Huenerbein, R.; Ehrlich, S. On the importance of the dispersion energy for the thermodynamic stability of molecules. *Chem. Phys. Chem* **2011**, *12*, 1258–1261.

[155] Grimme, S. Seemingly simple stereoelectronic effects in alkane isomers and the implications for Kohn–Sham density functional theory. *Angew. Chem. Intl. Ed.* **2006**, *45*, 4460–4464.

[156] Goerigk, L. How do DFT-DCP, DFT-NL, and DFT-D3 compare for the description of London-dispersion effects in conformers and general thermochemistry? *J. Chem. Theory Comput.* **2014**, *10*, 968–980.

[157] Holmes, J. D.; Otero-de-la-Roza, A.; DiLabio, G. A. Accurate modeling of water clusters with density-functional theory usin g atom-centered potentials. *J. Chem. Theory Comput.* **2017**, *13*, 4205–4215.

Correction to BH9, a New Comprehensive Benchmark Dataset for Barrier Heights and Reaction Energies: Assessment of Density Functional Approximations and Basis Set Incompleteness Potentials

Viki Kumar Prasad,[1, *] Zhipeng Pei,[1] Simon Edelmann,[1, †] Alberto Otero-de-la-Roza,[2, ‡] and Gino A. DiLabio[1, §]

[1] Department of Chemistry, University of British Columbia,
3247 University Way, Kelowna, British Columbia, Canada V1V 1V7
[2] Departamento de Química Física y Analítica and MALTA Consolider Team,
Facultad de Química, Universidad de Oviedo, 33006 Oviedo, Spain
(Dated: April 11, 2022)

The reference data for a few barrier heights and reaction energies in our original article[1] were incorrect due to convergence of the self-consistent-field (SCF) energy to spurious minima. The systems affected are from the following reactions (see Table I in the original article[1]):

- Radical rearrangement and addition (I): reactions 41 (P), 45 (TS), and 47 (P).

- Halogen atom transfer (III): reactions 9 (R and TS), 16 (R and TS), and 19 (R and TS)

- Hydrogen atom transfer (IV): reactions 32 (TS), 33 (TS), 34 (TS), 40 (TS), 75 (TS), 80 (R and TS), 86 (TS), and 88 (TS).

where the "R", "P", and "TS" abbreviations stand for reactant, product, and transition state, and indicate the molecules affected. In addition, the reference energies used for the DFT comparison in the original article were DLPNO-CCSD(T)/aug-cc-pVTZ instead of the focal-point data.

New reference data is provided in the Supporting Information accompanying this correction. The figures and tables in the original article are slightly modified because of the change in reference energies. In particular,

- Table IV in the original article is replaced by Table I.

- Table V in the original article is replaced by Table II.

- Figure 1 in the original article is replaced by Figure 1.

- Figure 2 in the original article is replaced by Figure 2.

- Table VI in the original article is replaced by Table III. Only the comparison of the considered methods with the reference has changed significantly; the comparison with the complete-basis-set (CBS) data is almost unaffected.

All claims made in the discussion and conclusions are still valid with the new results. In particular, the

FIG. 1. Barrier height vs. reaction energy mean absolute errors (MAE) for the chosen functionals. Open symbols represent the XDM-corrected version of each functional.
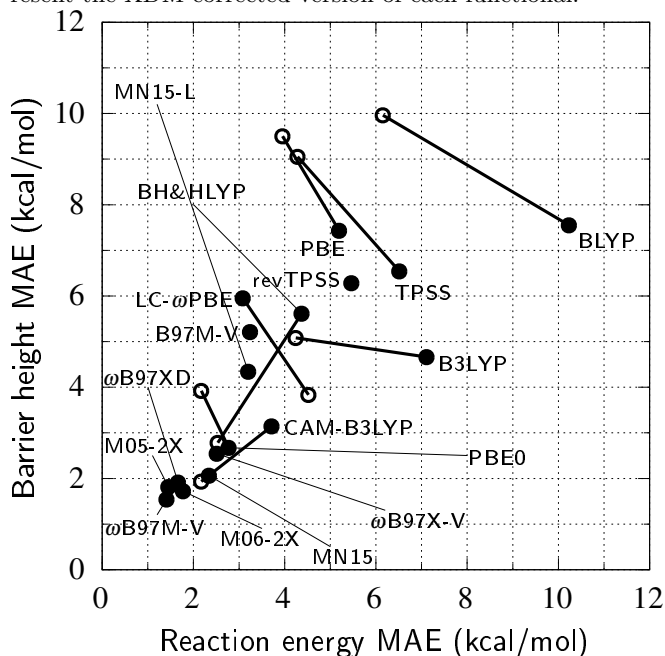
best-performing functional is still ωB97M-V, and the best-performing semilocal (meta-GGA) functional is MN15-L.

TABLE I. Average errors in the BH9 reaction energies using various density functionals.[a]

Functional		I	II	III	IV	V	VI	VII	VIII	IX	Total
BLYP	MAE	7.85	20.68	6.08	2.96	2.33	10.29	2.67	3.67	9.76	10.23
	ME	7.85	19.34	-3.01	-1.27	0.09	9.41	0.65	-0.97	9.76	7.62
BLYP-XDM	MAE	4.69	12.28	5.12	2.61	2.26	2.70	2.55	3.32	3.64	6.15
	ME	4.67	10.89	-2.34	-1.20	0.07	1.94	0.42	-1.06	3.48	3.76
PBE	MAE	2.67	8.90	6.03	3.01	2.64	4.42	2.86	3.69	3.00	5.19
	ME	0.99	7.73	-3.20	-1.05	1.61	3.61	0.29	-1.48	1.37	2.47
PBE-XDM	MAE	2.05	6.00	5.68	2.91	2.65	1.37	2.85	3.80	3.31	3.95
	ME	0.11	4.74	-2.97	-1.04	1.57	0.19	0.23	-1.62	-1.06	1.05
TPSS	MAE	3.44	12.19	5.66	2.97	2.66	6.82	2.33	3.44	4.41	6.51
	ME	2.39	11.21	-2.81	-0.91	1.32	5.95	0.45	-1.43	4.41	4.10
TPSS-XDM	MAE	2.16	7.25	5.07	2.83	2.72	2.31	2.29	3.02	2.57	4.28
	ME	0.69	6.17	-2.41	-0.88	1.32	0.93	0.33	-1.56	0.56	1.77
revTPSS	MAE	2.65	9.29	5.14	3.47	3.04	6.12	1.97	3.47	3.00	5.46
	ME	0.65	8.30	-2.45	-0.79	1.67	5.31	0.43	-1.55	2.68	2.95
MN15-L	MAE	1.69	4.22	3.93	2.18	3.87	2.94	2.52	2.55	2.61	3.20
	ME	-0.61	2.95	-1.95	-1.01	-2.90	-1.47	-0.10	-1.37	-0.20	0.02
B97M-V	MAE	1.70	5.09	3.81	2.30	2.70	1.66	1.96	2.36	2.47	3.24
	ME	0.13	3.88	-1.98	-0.95	-1.95	-0.33	0.05	-0.76	-0.34	0.59
B3LYP	MAE	5.06	14.06	4.40	2.17	2.33	7.51	1.66	2.43	6.95	7.11
	ME	5.05	13.13	-1.72	-0.94	-1.58	6.77	0.39	-0.47	6.95	5.06
B3LYP-XDM	MAE	3.11	8.26	3.71	1.88	2.27	1.81	1.61	2.01	2.55	4.24
	ME	3.05	7.27	-1.26	-0.90	-1.60	1.03	0.25	-0.63	2.41	2.35
PBE0	MAE	2.15	4.04	3.50	1.94	1.46	2.71	1.62	2.16	1.75	2.77
	ME	-1.38	2.28	-2.30	-0.49	-0.41	2.01	0.01	-0.78	-0.16	0.33
PBE0-XDM	MAE	2.30	2.28	3.14	1.81	1.33	1.79	1.62	2.08	3.13	2.17
	ME	-2.23	-0.67	-2.08	-0.49	-0.43	-1.40	-0.04	-0.91	-2.56	-1.07
BH&HLYP	MAE	2.90	7.77	2.23	1.78	3.69	4.92	0.82	1.89	4.34	4.37
	ME	2.76	7.16	-1.11	-0.34	-2.93	4.25	0.23	0.47	4.34	2.68
BH&HLYP-XDM	MAE	1.72	3.81	1.81	1.56	3.56	2.44	0.81	1.47	1.37	2.53
	ME	1.44	2.96	-0.79	-0.32	-2.92	-0.22	0.14	0.34	1.02	0.72
M05-2X	MAE	1.02	1.73	1.75	0.92	2.16	1.28	0.73	1.62	1.29	1.45
	ME	-0.29	0.68	-0.15	-0.46	-1.56	-0.28	-0.29	-0.16	-0.33	-0.13
M06-2X	MAE	1.68	2.53	1.94	1.29	1.06	1.51	0.80	1.73	1.03	1.77
	ME	-0.06	2.09	-0.46	-0.66	-0.49	0.58	-0.36	-0.75	0.28	0.45
MN15	MAE	1.44	2.73	3.24	1.57	3.78	2.31	1.73	1.88	1.22	2.34
	ME	-0.77	1.64	-1.26	-0.81	-2.95	-0.14	-0.33	-0.87	0.11	-0.17
CAM-B3LYP	MAE	2.37	6.73	2.41	1.42	2.22	4.53	0.93	1.49	3.57	3.71
	ME	2.15	6.21	-1.54	-0.55	-1.51	3.93	0.35	-0.12	3.57	2.28
CAM-B3LYP-XDM	MAE	1.49	3.46	1.98	1.21	2.17	1.91	0.93	1.28	1.37	2.17
	ME	1.14	2.80	-1.27	-0.54	-1.55	0.02	0.28	-0.30	0.72	0.66
LC-ωPBE	MAE	4.33	5.03	3.08	1.47	1.64	1.95	1.13	1.34	1.40	3.08
	ME	-4.24	-4.20	-1.14	-0.21	1.08	0.51	0.55	0.01	-1.07	-1.82
LC-ωPBE-XDM	MAE	5.40	8.45	2.71	1.47	1.62	4.05	1.12	1.38	3.65	4.52
	ME	-5.40	-7.80	-0.87	-0.19	1.22	-3.21	0.47	0.02	-3.65	-3.47
ωB97XD	MAE	1.25	1.75	2.50	1.60	0.94	2.47	1.19	1.19	1.28	1.66
	ME	-0.49	0.42	-1.33	-0.51	-0.03	-1.59	0.28	-0.41	0.16	-0.28
ωB97X-V	MAE	2.41	3.81	2.32	1.75	0.82	3.04	0.95	1.01	2.15	2.51
	ME	-2.41	-3.50	-0.88	-0.36	0.14	-2.06	0.30	-0.17	-2.14	-1.78
ωB97M-V	MAE	1.07	1.44	1.58	1.29	1.33	2.39	0.73	1.08	1.21	1.41
	ME	-0.83	-1.06	-0.97	-0.61	-0.80	-1.63	-0.12	-0.26	-0.78	-0.90

[a] Units are kcal/mol. MAE = mean absolute error. ME = mean error. The roman numerals represent the reaction types in Table I of the original article.

TABLE II. Average errors in the BH9 barrier heights using various density functionals.[a]

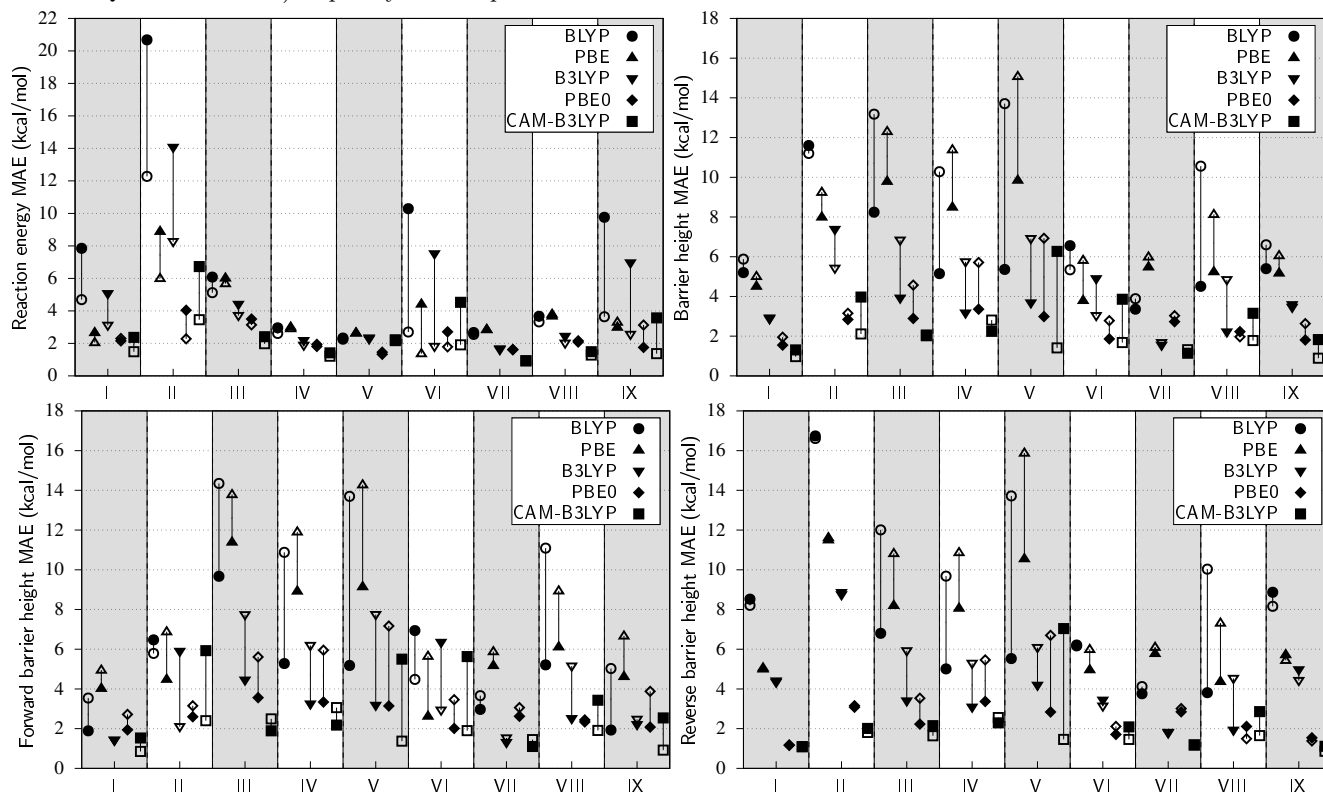| Functional		I	II	III	IV	V	VI	VII	VIII	IX	Total
BLYP	MAE	5.20	11.60	8.24	5.15	5.36	6.56	3.36	4.51	5.40	7.55
	ME	−4.59	−7.03	−7.78	−3.76	−2.74	1.29	−1.91	−3.94	−3.99	−4.74
BLYP-XDM	MAE	5.88	11.20	13.18	10.28	13.71	5.34	3.89	10.56	6.60	9.96
	ME	−5.88	−11.17	−13.18	−10.28	−13.45	−4.52	−3.87	−10.56	−6.42	−9.85
PBE	MAE	4.52	8.00	9.80	8.50	9.86	3.80	5.49	5.25	5.18	7.43
	ME	−4.51	−7.64	−9.80	−8.41	−9.60	−2.92	−5.21	−5.12	−5.04	−7.19
PBE-XDM	MAE	5.01	9.25	12.31	11.39	15.08	5.82	5.99	8.13	6.06	9.50
	ME	−5.01	−9.25	−12.31	−11.39	−14.99	−5.75	−5.99	−8.13	−5.97	−9.48
TPSS	MAE	4.43	8.82	7.81	5.55	6.07	4.55	3.81	5.10	4.71	6.54
	ME	−4.34	−7.51	−7.70	−4.87	−4.84	−1.56	−2.98	−4.97	−4.39	−5.58
TPSS-XDM	MAE	5.15	10.14	11.35	9.32	12.70	5.68	4.22	9.42	5.96	9.05
	ME	−5.15	−10.14	−11.35	−9.32	−12.50	−5.59	−4.20	−9.42	−5.89	−9.02
revTPSS	MAE	4.50	8.09	8.13	5.36	6.00	4.55	3.11	5.33	4.56	6.28
	ME	−4.48	−7.64	−7.98	−4.72	−5.09	−2.58	−2.18	−5.28	−4.38	−5.73
MN15-L	MAE	1.75	4.18	4.61	5.07	9.01	3.77	2.68	2.23	2.00	4.34
	ME	−1.04	−3.50	−3.41	−4.59	−8.79	−3.49	1.00	−1.39	−1.25	−3.64
B97M-V	MAE	2.40	4.77	7.51	6.20	10.17	2.76	1.38	4.37	2.83	5.21
	ME	−2.32	−4.54	−7.36	−6.19	−9.99	−2.58	−0.78	−4.37	−2.67	−5.06
B3LYP	MAE	2.91	7.37	3.91	3.16	3.67	4.89	1.54	2.21	3.58	4.66
	ME	−1.87	−1.99	−2.39	−0.72	1.78	2.77	−0.24	0.17	−1.48	−0.89
B3LYP-XDM	MAE	2.87	5.42	6.83	5.74	6.91	3.03	1.67	4.84	3.45	5.08
	ME	−2.80	−5.01	−6.49	−5.74	−6.76	−1.79	−1.63	−4.84	−3.22	−4.79
PBE0	MAE	1.55	2.84	2.89	3.36	2.99	1.86	2.73	2.23	1.81	2.67
	ME	−1.11	−1.14	−2.08	−2.74	−1.50	0.11	−2.26	1.08	−1.54	−1.46
PBE0-XDM	MAE	1.95	3.15	4.57	5.71	6.93	2.78	3.03	1.97	2.63	3.92
	ME	−1.60	−2.75	−4.57	−5.71	−6.92	−2.73	−3.03	−1.90	−2.46	−3.74
BH&HLYP	MAE	1.88	6.14	5.37	5.23	11.46	5.79	3.02	5.20	2.83	5.61
	ME	1.42	5.58	5.37	5.01	11.46	5.72	3.02	5.13	2.53	5.32
BH&HLYP-XDM	MAE	1.19	3.82	2.27	2.05	4.46	2.78	2.01	1.96	1.45	2.78
	ME	0.72	3.32	2.13	1.05	4.45	2.06	1.96	1.22	1.23	2.26
M05-2X	MAE	1.11	1.65	2.51	1.71	3.29	1.67	1.24	1.71	1.20	1.81
	ME	−0.80	−0.95	0.07	−1.43	2.67	−0.93	−0.67	0.41	−1.11	−0.55
M06-2X	MAE	1.18	1.57	1.98	2.30	2.13	1.44	1.15	1.55	1.11	1.72
	ME	0.23	−0.18	0.72	−2.10	1.41	−1.09	−0.56	0.91	−0.82	−0.36
MN15	MAE	1.10	1.98	2.82	2.42	2.50	2.47	1.41	1.60	0.98	2.06
	ME	−0.45	−0.98	0.58	−1.65	−1.20	−2.28	−0.72	0.26	−0.55	−0.96
CAM-B3LYP	MAE	1.31	3.97	2.02	2.24	6.27	3.86	1.14	3.15	1.83	3.14
	ME	0.36	2.77	0.97	0.68	6.01	3.60	−0.19	2.80	0.76	2.11
CAM-B3LYP-XDM	MAE	0.97	2.11	2.06	2.81	1.41	1.68	1.32	1.78	0.89	1.93
	ME	−0.20	0.93	−1.78	−2.65	0.09	0.40	−1.04	−0.54	−0.28	−0.45
LC-ωPBE	MAE	2.95	8.06	7.00	3.21	10.72	3.98	1.23	8.53	3.21	5.95
	ME	2.67	8.03	7.00	2.87	10.34	3.73	−0.22	8.53	3.10	5.75
LC-ωPBE-XDM	MAE	2.74	6.18	4.04	1.34	4.39	2.48	1.38	5.03	2.59	3.83
	ME	2.05	6.04	4.00	−0.67	3.83	0.64	−1.24	5.03	1.92	3.01
ωB97XD	MAE	0.88	1.66	2.63	3.07	1.75	1.79	0.70	1.79	0.92	1.91
	ME	−0.18	1.17	0.59	−2.99	−1.57	−0.66	−0.31	0.94	0.05	−0.37
ωB97X-V	MAE	1.34	3.54	2.70	2.06	3.34	1.85	0.68	2.01	1.44	2.54
	ME	0.63	3.48	1.20	−1.89	3.05	0.19	−0.33	1.67	0.97	1.29
ωB97M-V	MAE	0.71	1.27	1.24	2.03	3.17	1.73	0.55	1.60	0.83	1.54
	ME	−0.02	0.97	−0.72	−1.71	2.62	−1.11	−0.28	−0.18	0.04	0.04

[a] Units are kcal/mol. MAE = mean absolute error. ME = mean error. The roman numerals represent the reaction types in Table I.

[*] ORCID:0000-0003-0982-3129

[†] Current address: Department of Chemistry, McGill Uni-

TABLE III. Mean absolute errors (MAE) for the BH9 barrier heights and reaction energies of PBE0-XDM with several BSIP-corrected and uncorrected basis sets.[a]

		Reaction energies		Barrier heights	
		CBS[b]	Ref.[c]	CBS[b]	Ref.[c]
6-31G∗	Bare	3.59	4.49	2.46	5.52
	BSIP	1.91	2.68	1.62	4.11
6-31+G∗	Bare	2.49	3.31	1.48	4.55
	BSIP	0.89	2.08	0.75	3.96
6-31+G∗∗	Bare	1.81	2.85	1.42	4.75
	BSIP	0.63	2.07	0.63	3.92
Def2-SV(P)	Bare	4.12	5.09	3.11	6.18
	BSIP	1.95	2.87	1.80	3.58
Def2-SVP	Bare	3.12	4.30	2.90	6.10
	BSIP	2.19	3.20	1.74	3.62
pc-1	Bare	2.42	3.31	2.60	6.10
	BSIP	1.41	2.52	1.32	4.17
Def2-QZVPP			2.74		2.85

[a] Units are kcal/mol. The statistics correspond to the whole BH9 set. [b] CBS = MAEs calculated with respect to our complete-basis-set estimate (Def2-QZVPP).
[c] Ref. = MAEs calculated with respect to the DLPNO-CCSD(T)/CBS reference data for the BH9.